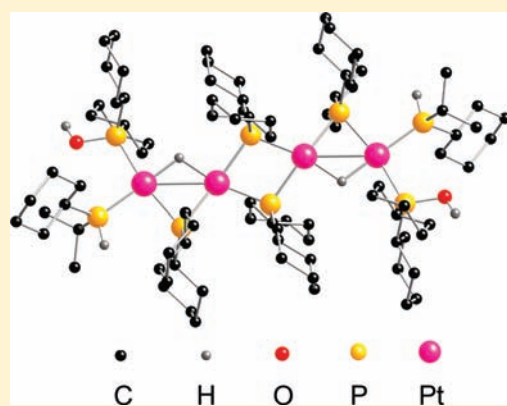


Hydrido Phosphanido Bridged Polynuclear Complexes Obtained by Protonation of a Phosphinito Bridged Pt(I) Complex with HBF<sub>4</sub> and HFMario Latronico,<sup>†</sup> Piero Mastrorilli,<sup>\*,†</sup> Vito Gallo,<sup>†</sup> Maria Michela Dell'Anna,<sup>†</sup> Francesco Creati,<sup>‡</sup> Nazzareno Re,<sup>‡</sup> and Ulli Englert<sup>§</sup><sup>†</sup>Dipartimento di Ingegneria delle Acque e di Chimica del Politecnico di Bari, via Orabona 4, I-70125 Bari, Italy<sup>‡</sup>Dipartimento di Scienze del Farmaco, Università "G. d'Annunzio", Via dei Vestini 31, 06100 Chieti, Italy<sup>§</sup>Institut für Anorganische Chemie der RWTH, Landoltweg 1, D-52074 Aachen, Germany

Supporting Information

**ABSTRACT:** The protonation of the phosphinito-bridged Pt(I) complex [(PHCY<sub>2</sub>)Pt(μ-PCY<sub>2</sub>){κ<sup>2</sup>P,O-μ-P(O)CY<sub>2</sub>}Pt(PHCY<sub>2</sub>)](Pt–Pt) (**1**) by aqueous HBF<sub>4</sub> or hydrofluoric acid leads selectively to the hydrido-bridged solvento species *syn*-[(PHCY<sub>2</sub>)(H<sub>2</sub>O)Pt(μ-PCY<sub>2</sub>)(μ-H)Pt(PHCY<sub>2</sub>){κP-P(OH)CY<sub>2</sub>}]<sub>2</sub>(Y)<sub>2</sub>(Pt–Pt) ([2-H<sub>2</sub>O]Y<sub>2</sub>) {Y = BF<sub>4</sub>, F(HF)<sub>*n*</sub>} when an excess of acid was used. On standing in halogenated solvents, complex [2-H<sub>2</sub>O](BF<sub>4</sub>)<sub>2</sub> undergoes a slow but complete isomerization to [(PHCY<sub>2</sub>)<sub>2</sub>Pt(μ-PCY<sub>2</sub>)(μ-H)Pt{κP-P(OH)CY<sub>2</sub>}(H<sub>2</sub>O)](BF<sub>4</sub>)<sub>2</sub>(Pt–Pt) ([4-H<sub>2</sub>O][BF<sub>4</sub>]<sub>2</sub>) having the P(OH)CY<sub>2</sub> ligand *trans* to the hydride. The water molecule coordinated to platinum in [2-H<sub>2</sub>O][BF<sub>4</sub>]<sub>2</sub> is readily replaced by halides, nitriles, and triphenylphosphane, and the acetonitrile complex [2-CH<sub>3</sub>CN][BF<sub>4</sub>]<sub>2</sub> was characterized by XRD analysis. Solvento species other than aqua complexes, such as [2-acetone-*d*<sub>6</sub>]<sup>2+</sup> or [2-CD<sub>2</sub>Cl<sub>2</sub>]<sup>2+</sup> were obtained in solution by the reaction of excess etherate HBF<sub>4</sub> with **1** in the relevant solvent. The complex [2-H<sub>2</sub>O](Y)<sub>2</sub> [Y = F(HF)<sub>*n*</sub>] spontaneously isomerizes into the terminal hydrido complexes [(PHCY<sub>2</sub>)Pt(μ-PCY<sub>2</sub>){κ<sup>2</sup>P,O-μ-P(O)CY<sub>2</sub>}Pt(H)(PHCY<sub>2</sub>)](Y)(Pt–Pt) ([6](Y)). In the presence of HF, complex [6](Y) transforms into the bis-phosphanido-bridged Pt(II) dinuclear complex [(PHCY<sub>2</sub>)(H)Pt(μ-PCY<sub>2</sub>)<sub>2</sub>Pt{κP-P(OH)CY<sub>2</sub>}]<sub>2</sub>(Y)(Pt–Pt) ([7](Y)). When the reaction of **1** with HF was carried out with diluted hydrofluoric acid by allowing the HF to slowly diffuse into the dichloromethane solution, the main product was the linear 60e tetranuclear complex [(PHCY<sub>2</sub>){κP-P(O)CY<sub>2</sub>}Pt<sup>1</sup>(μ-PCY<sub>2</sub>)(μ-H)Pt<sup>2</sup>(μ-PCY<sub>2</sub>)<sub>2</sub>(Pt<sup>1</sup>–Pt<sup>2</sup>)]<sub>2</sub> (**8**). Insoluble compound **8** is readily protonated by HBF<sub>4</sub> in dichloromethane, forming the more soluble species [(PHCY<sub>2</sub>){κP-P(OH)CY<sub>2</sub>}Pt<sup>1</sup>(μ-PCY<sub>2</sub>)(μ-H)Pt<sup>2</sup>(μ-PCY<sub>2</sub>)<sub>2</sub>](BF<sub>4</sub>)<sub>2</sub>(Pt<sup>1</sup>–Pt<sup>2</sup>) { [9][BF<sub>4</sub>]<sub>2</sub>}. XRD analysis of [9][BF<sub>4</sub>]<sub>2</sub>·2CH<sub>2</sub>Cl<sub>2</sub> shows that [9]<sup>2+</sup> is comprised of four coplanar Pt atoms held together by four phosphanido and two hydrido bridges. Both XRD and NMR analyses indicate alternate intermetal distances with peripheral Pt–Pt bonds and a longer central Pt···Pt separation. DFT calculations allow tracing of the mechanistic pathways for the protonation of **1** by HBF<sub>4</sub> and HF and evaluation of their energetic aspects. Our results indicate that in both cases the protonation occurs through an initial proton transfer from the acid to the phosphinito oxygen, which then shuttles the incoming proton to the Pt–Pt bond. The different evolution of the reaction with HF, leading also to [6](Y) or **8**, has been explained in terms of the peculiar behavior of the F(HF)<sub>*n*</sub><sup>–</sup> anions and their strong basicity for *n* = 0 or 1.



## INTRODUCTION

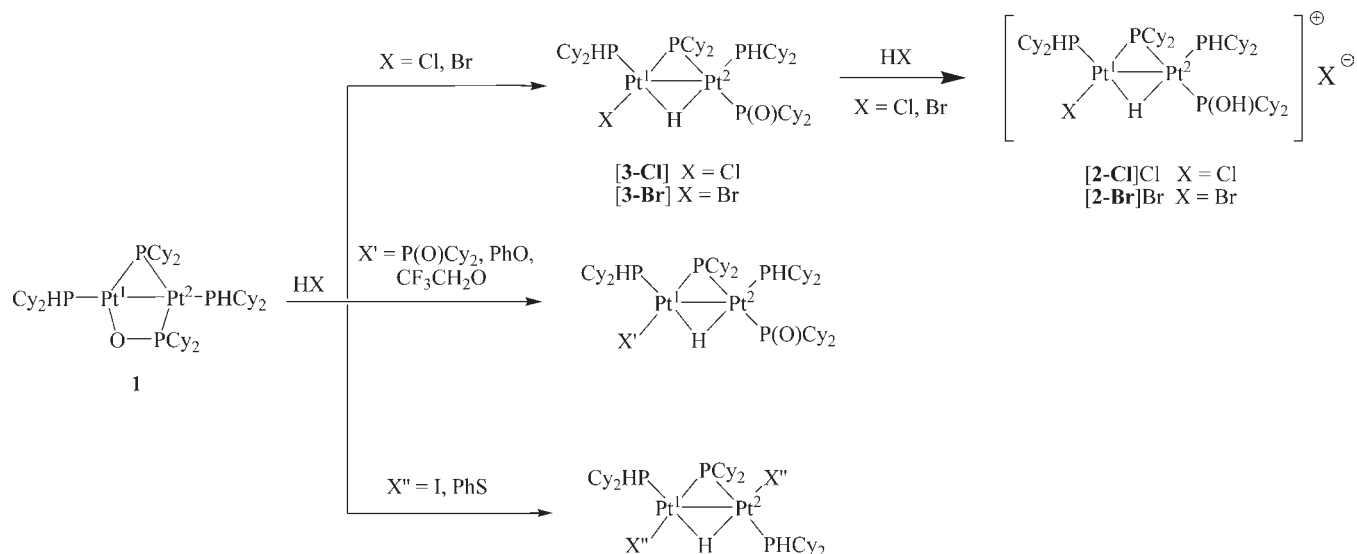
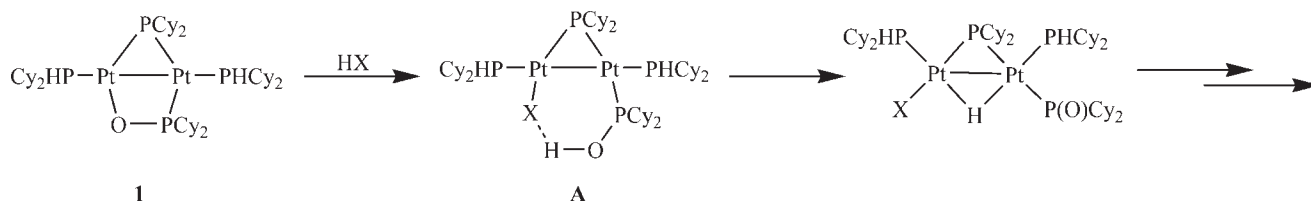
The phosphinito-bridged complex [(PHCY<sub>2</sub>)Pt(μ-PCY<sub>2</sub>)-{κ<sup>2</sup>P,O-μ-P(O)CY<sub>2</sub>}Pt(PHCY<sub>2</sub>)](Pt–Pt) (**1**)<sup>1</sup> represents an attractive molecule due to the presence of the Pt–O fragment, which imparts a multifaceted reactivity comprising substitution,<sup>2</sup> addition,<sup>3</sup> and H<sub>2</sub> activation.<sup>4</sup> The protonation of **1** by Brønsted acids such as HCl, HBr, HI, PhOH, P(OH)CY<sub>2</sub>, CF<sub>3</sub>CH<sub>2</sub>OH, and PhSH resulted in all cases in bridging hydrido diplatinum complexes<sup>5</sup> as shown in Scheme 1.

It is apparent from Scheme 1 that HCl and HBr give first the monoprotonated compounds [(PHCY<sub>2</sub>)(X)Pt(μ-PCY<sub>2</sub>)(μ-H)Pt(PHCY<sub>2</sub>){κP-P(O)CY<sub>2</sub>}]<sub>2</sub>(Pt–Pt) and then, in the presence of

excess acid, [(PHCY<sub>2</sub>)(X)Pt(μ-PCY<sub>2</sub>)(μ-H)Pt(PHCY<sub>2</sub>){κP-P(OH)CY<sub>2</sub>}]<sub>2</sub>X (Pt–Pt) (X = Cl or Br). On the other hand, the protonation of **1** by weaker acids such as dicyclohexylphosphane oxide, phenol, or 1,1,1-trifluoroethanol stops at the monoprotonated species [(PHCY<sub>2</sub>)(X')Pt(μ-PCY<sub>2</sub>)(μ-H)Pt(PHCY<sub>2</sub>){κP-P(O)CY<sub>2</sub>}]<sub>2</sub>(Pt–Pt) (X' = P(O)CY<sub>2</sub>, PhO, or CF<sub>3</sub>CH<sub>2</sub>O) even when a strong excess of protonating agent is used. Notably, both HI and PhSH give, as final products, the *anti*-[(PHCY<sub>2</sub>)(X'')Pt(μ-PCY<sub>2</sub>)(μ-H)Pt(PHCY<sub>2</sub>)(X'')]<sub>2</sub>(Pt–Pt)

Received: December 10, 2010

Published: March 17, 2011

Scheme 1. Reactivity of **1** with Brønsted Acids Having Coordinating AnionsScheme 2. Mechanism of Protonation of **1** by HX ( $\text{X} = \text{Cl, Br, I, SPh}$ )

( $\text{X}'' = \text{I}$  or  $\text{PhS}$ ) complexes, featuring two  $\text{X}''$  residues covalently bound to the Pt atoms.

These findings indicate that the product of the protonation of **1** depends on both the acid strength of the HX molecule and on the affinity to platinum of the X residue. In fact, HI and PhSH, two Brønsted acids endowed with very different acid strengths but having in common a residue characterized by a strong affinity to platinum, gave isostructural products (Scheme 1). A mechanistic study based on NMR data and DFT calculations revealed that the kinetic protonation site is the phosphinito oxygen which shuttles the incoming proton to the Pt–Pt bond. The reaction was shown to pass through the formation of a six-membered platinacycle complex **A** detected in solution by NMR spectroscopy when less than 1 equiv of HX ( $\text{X} = \text{Cl, Br, I, SPh}$ ) was reacted with **1**<sup>3,6</sup> (Scheme 2).

A common feature for all reactions shown in Scheme 1 is that the X residues possess a fair to good coordinating ability toward Pt, thus forming in all products a covalent bond with the electrophilic<sup>2</sup> Pt<sup>1</sup> atom (the one originally bearing the phosphinito oxygen).

In order to investigate the protonation of **1** with Brønsted acids whose anion possesses *poor coordinating ability* toward Pt, we decided to study the reaction of **1** with  $\text{HBF}_4$  and with HF, which led to new dinuclear or tetranuclear hydrido phosphanido-bridged Pt complexes.

## RESULTS AND DISCUSSION

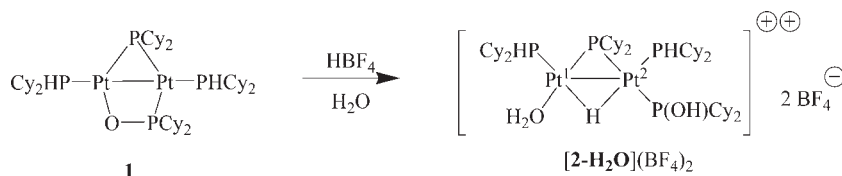
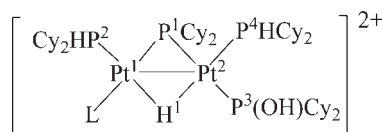
**Reaction with  $\text{HBF}_4$ .** The addition of excess (>2 equiv) aqueous  $\text{HBF}_4$  to an *n*-hexane solution of **1** causes the immediate

precipitation of the dicationic hydrido-bridged aqua complex *syn*-[( $\text{PHCy}_2$ )( $\text{H}_2\text{O}$ )Pt( $\mu\text{-PCy}_2$ )( $\mu\text{-H}$ )Pt( $\text{PHCy}_2$ ){ $\kappa\text{P-P(OH)-Cy}_2$ }] $(\text{BF}_4)_2$  (*Pt–Pt*) ([2- $\text{H}_2\text{O}$ ][ $\text{BF}_4$ ]<sub>2</sub>), which represents the product of double protonation of **1** (Scheme 3). The structure of [2- $\text{H}_2\text{O}$ ]<sup>2+</sup> is similar to that of the reaction products of **1** with excess HCl or HBr ([2-Cl]<sup>+</sup> or [2-Br]<sup>+</sup> respectively, Scheme 1), the only differences being the water ligand in place of the halide bonded to Pt<sup>1</sup> and, as a consequence, the charge of the cationic complex.

As expected, <sup>31</sup>P and <sup>195</sup>Pt NMR spectroscopic features of the aqua complex [2- $\text{H}_2\text{O}$ ]<sup>2+</sup> (Table 1) resemble those of the cationic complexes [( $\text{PHCy}_2$ )(X)Pt( $\mu\text{-PCy}_2$ )( $\mu\text{-H}$ )Pt( $\kappa\text{P-P(OH)-Cy}_2$ )] $(\text{BF}_4)_2$  (*Pt–Pt*) ([2- $\text{H}_2\text{O}$ ][ $\text{BF}_4$ ]<sub>2</sub>) (X = Cl, Br, I)<sup>3</sup> and will be not discussed here. The <sup>1</sup>H NMR spectrum of [2- $\text{H}_2\text{O}$ ]<sup>2+</sup> recorded at 295 K in  $\text{CD}_2\text{Cl}_2$  showed, besides the cyclohexyl and the PH protons, a multiplet centered at  $\delta$  –5.48 attributable to the bridging hydride, and a very broad signal at  $\delta$  5.8 (Figure 1). On lowering the temperature down to 258 K, the latter signal splits into two broad signals at  $\delta$  5.34 and  $\delta$  6.33 ascribable to the protons of the coordinated water and of the POH moiety, respectively. These attributions are corroborated by the disappearance of the signal at  $\delta$  5.34 (but not of that at  $\delta$  6.33) upon the addition of acetonitrile to a  $\text{CD}_2\text{Cl}_2$  solution of [2- $\text{H}_2\text{O}$ ]<sup>2+</sup>.

The bridging hydride participates in exchange phenomena involving the protons of the coordinated water and of the coordinated P(OH)Cy<sub>2</sub>, as the addition of D<sub>2</sub>O to a  $\text{CD}_2\text{Cl}_2$  solution of [2- $\text{H}_2\text{O}$ ]<sup>2+</sup> caused the complete disappearance of the

Scheme 3

Table 1. NMR Features of Solvento Species  $[2-L]^{2+}$  ( $\delta$ 's are in ppm; coupling constants are in Hz)

complex <sup>a</sup>	L	$\delta$ P <sup>1</sup>	$\delta$ P <sup>2</sup>	$\delta$ P <sup>3</sup>	$\delta$ P <sup>4</sup>	$\delta$ H <sup>1</sup>	$\delta$ Pt <sup>1</sup>	$\delta$ Pt <sup>2</sup>	$^2J(P^1, P^3)$
$[2-H_2O]^{2+}$	H <sub>2</sub> O	149.7	9.1	126.8	-1.7	-5.48	-5302	-5589	289
$[2\text{-acetone-}d_6]^{2+b}$	acetone- <i>d</i> <sub>6</sub>	154.0	5.4	126.2	-3.7	-5.49	-5296	-5580	292
$[2\text{-CD}_2\text{Cl}_2]^{2+b}$	CD <sub>2</sub> Cl <sub>2</sub>	152.4	11.1	128.8	0.2	-5.50	-5292	-5576	297

<sup>a</sup> As a tetrafluoroborate salt. A more complete NMR characterization is reported in the Supporting Information. <sup>b</sup> Obtained in an NMR tube starting from **1** + HBF<sub>4</sub>·Me<sub>2</sub>O (>2 equiv) at room temperature in the corresponding coordinating solvent.

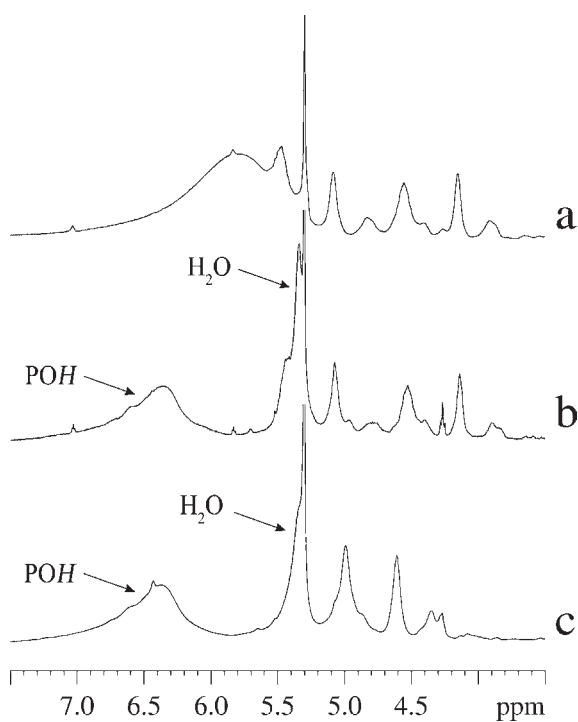


Figure 1. NMR spectra of  $[2-H_2O](BF_4)_2$  in  $CD_2Cl_2$ : (a)  $^1H$  NMR at 295 K; (b)  $^1H$  NMR at 258 K; (c)  $^1H\{^{31}P\}$  NMR at 258 K.

$^1H$  signals attributed to the POH, coordinated H<sub>2</sub>O, and bridging hydride.<sup>7</sup> This is in accordance with the acidic character of bridging hydrides bonded to (formally) Pt(II) centers.<sup>8</sup>

When the protonation of **1** in  $CH_2Cl_2$  was carried out using HBF<sub>4(aq)</sub> in amounts ranging from 1 to 2 equiv, only extremely broad signals were found in the  $^1H$  and  $^{31}P\{^1H\}$  NMR spectra over a wide range of temperatures, indicating the occurrence of

an equilibrium between the monocationic complex  $[3-H_2O]^+$  and the dicationic species  $[2-H_2O]^{2+}$  (Scheme 4), a result paralleling that obtained with HCl.<sup>3</sup>

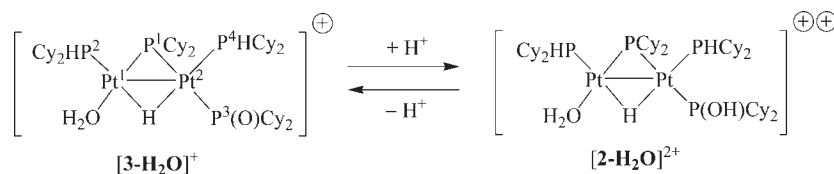
Differently from the cases of HCl, HBr, HI, and PhSH, when less than 1 equiv of HBF<sub>4</sub> was reacted with **1**, no traces of intermediates similar to **A** (Scheme 2) were detected in solution by NMR spectroscopy, even at low *T* (200 K).

While the related chlorido or bromido complexes  $[2-X]^+$  (*X* = Cl, Br) were found stable in solution (even in the presence of the corresponding halohydric acid),  $[2-H_2O]^{2+}$  spontaneously isomerizes to  $[(PHCv_2)_2Pt(\mu-PCv_2)(\mu-H)Pt\{\kappa P-P(OH)Cv_2\}-(H_2O)]^{2+}(Pt-Pt)$  ( $[4-H_2O]^{2+}$ , Scheme 5) when left in halogenated solvents. The conversion  $[2-H_2O]^{2+} \rightarrow [4-H_2O]^{2+}$  is slow but irreversible, being completed after 1 month in  $CD_2Cl_2$  at room temperature (rt), indicating that such transformation is thermodynamically favored. In the  $^{31}P\{^1H\}$  NMR spectrum of  $[4-H_2O]^{2+}$ , the bridging phosphanide P<sup>1</sup> is strongly coupled to the coordinated P<sup>3</sup>HCV<sub>2</sub> ( $^2J_{P(1),P(3)} = 229$  Hz) while the coordinated P<sup>4</sup>(OH)Cv<sub>2</sub> is coupled only to the coordinated P<sup>2</sup>HCV<sub>2</sub> ( $^3J_{P(2),P(4)} = 38$  Hz). The assignment of the structure depicted in Scheme 5 to  $[4-H_2O]^{2+}$  was possible by means of  $^1H-^{195}Pt$  HMQC (Figure 2) and  $^1H-^{31}P$  HMQC spectra, which indicated, *inter alia*, that the two PHCv<sub>2</sub> ligands are bonded to the same Pt<sup>1</sup> atom.

The complex  $[2-H_2O]^{2+}$  could be selectively obtained from the protonation of **1** only if fresh HBF<sub>4(aq)</sub> was used. The use of "aged" HBF<sub>4(aq)</sub> (which is known to be slowly hydrolyzed to HBF<sub>3</sub>OH)<sup>9</sup> gave a mixture containing variable amounts of  $[(PHCv_2)_2\{B(OH)F_3\}Pt(\mu-PCv_2)(\mu-H)Pt(PHCv_2)\{\kappa P-P(OH)Cv_2\}]BF_4(Pt-Pt)$  ( $[2-B(OH)F_3][BF_4]$ ).<sup>10</sup>

The complex  $[2-H_2O]^{2+}$  slowly decomposes in solution in the presence of excess HBF<sub>4</sub>, giving rise to fragmentation of the dinuclear core with the formation, after one week, of several products, among which the mononuclear Pt(II) species *cis*- $[Pt(H)\{\kappa P-P(OH)Cv_2\}(PHCv_2)_2][BF_4]$  ( $[5][BF_4]$ ) was identified.<sup>11</sup>

Scheme 4



Scheme 5

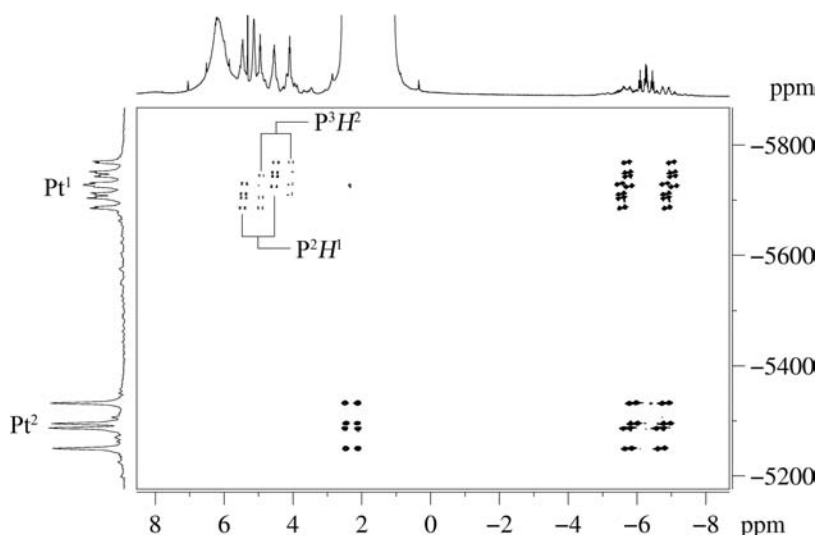
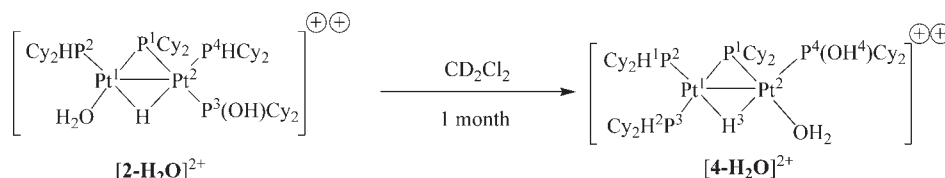


Figure 2.  $^1\text{H}$ – $^{195}\text{Pt}$  HMQC spectrum of  $[\text{4-H}_2\text{O}]^{2+}$  ( $\text{CD}_2\text{Cl}_2$ , 295 K).

When the protonation of **1** by  $\text{HBF}_4$  was carried out using etherate (instead of aqueous)  $\text{HBF}_4$  in coordinating solvents such as acetone- $d_6$  or  $\text{CD}_2\text{Cl}_2$ , different solvento species quantitatively formed,<sup>12</sup> whose main NMR features are listed in Table 1.

The coordinated solvent molecule of complexes  $[\text{2-L}]^{2+}$  is readily displaced by stronger ligands such as  $\text{Cl}^-$ ,  $\text{Br}^-$ , organonitriles, or  $\text{PPh}_3$ . The quantitative transformation of  $[\text{2-H}_2\text{O}]^{2+}$  into the corresponding chlorido or bromido complexes  $[\text{2-X}]^+$  ( $\text{X} = \text{Cl}, \text{Br}$ )<sup>3</sup> was observed when solid  $\text{NaCl}$  or  $\text{KBr}$  was added to a  $\text{CH}_2\text{Cl}_2$  solution of  $[\text{2-H}_2\text{O}]^{2+}$  at rt.

The addition of acetonitrile or benzonitrile to  $[\text{2-H}_2\text{O}]^{2+}$  in chloroform at rt immediately caused a ligand exchange with the formation of the RCN adducts shown in Scheme 6.

Differently from the solvento species listed in Table 1, which gave quite broad NMR signals at rt, complexes  $[\text{2-CH}_3\text{CN}]^{2+}$  and  $[\text{2-PhCN}]^{2+}$  are characterized by sharp  $^{195}\text{Pt}$ ,  $^{31}\text{P}$  (Figures S5, S6, S8, and S9, Supporting Information), and  $^1\text{H}$  NMR signals at rt, presumably as a consequence of the lesser lability of the ligand *trans* to  $\mu\text{-P}$  bonded to  $\text{Pt}^1$ . The  $^1\text{H}$  hydride as well as

the  $^{195}\text{Pt}$  NMR resonances of  $[\text{2-CH}_3\text{CN}]^{2+}$  and  $[\text{2-PhCN}]^{2+}$  are all slightly high-field shifted with respect to those of the starting complex  $[\text{2-H}_2\text{O}]^{2+}$ .

The XRD structure of  $[\text{2-CH}_3\text{CN}]^{2+}$  is shown in Figure 3 and resembles those already reported for the related complexes  $[\text{2-X}]^+$  ( $\text{X} = \text{Cl}, \text{Br}$ ).<sup>3</sup> In the dication  $[\text{2-CH}_3\text{CN}]^{2+}$ , the two Pt atoms are linked by a metal–metal bond of 2.8239(4) Å and bridged by a phosphanide subtending a Pt–P–Pt angle of 77.03(6)°. The coordination planes around each platinum are almost coplanar with a dihedral angle of 7.2(7)°. The H directly bonded to P4 forms an intramolecular hydrogen bond with the oxygen, as already found for  $[\text{2-X}]^+$  ( $\text{X} = \text{Cl}, \text{Br}$ ).<sup>3</sup> The hydroxyl H of the  $\text{P}(\text{OH})\text{Cy}_2$  ligand forms a hydrogen bond with one of the  $\text{BF}_4^-$  anions with  $\text{H}\cdots\text{F} = 1.85$  Å and  $\text{O-H}\cdots\text{F} = 158^\circ$ . The Pt1–N distance of 2.083(6) Å is perfectly in line with that of other acetonitrile Pt(II) complexes.<sup>13</sup> After completion of the structure model for  $[\text{2-CH}_3\text{CN}]^{2+}$  with the exception of the bridging hydride, a difference Fourier synthesis revealed a local electron density maximum of  $1 \text{ e} \cdot \text{Å}^{-3}$  at a distance of ca. 2 Å for Pt2 and 1.2 Å for Pt1. When a similarity restraint for equal Pt–H

Scheme 6

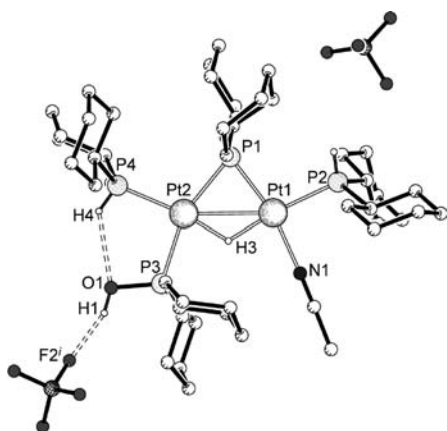
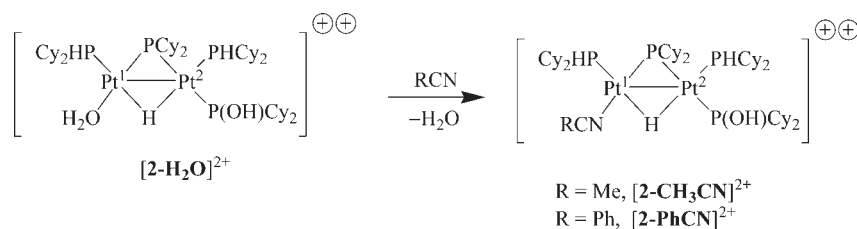


**Figure 3.** PLATON<sup>15</sup> drawing of  $[\text{2-CH}_3\text{CN}](\text{BF}_4)_2$ . Hydrogen atoms bonded to C have been omitted for clarity. Interatomic distances (Å) and angles (deg): Pt1–Pt2 = 2.8239(4), Pt1–P1 = 2.275(18), Pt1–P2 = 2.2617(19), Pt1–N1 = 2.083(7), Pt1–H3 = 1.66(2), Pt2–P1 = 2.3063(18), Pt2–P3 = 2.302(2), Pt2–P4 = 2.271(2), Pt2–H3 = 1.64(3), P3–O1 = 1.596(6), N(1)–C(25) = 1.143(9), Pt1–P1–Pt2 = 77.03(6), Pt1–H3–Pt2 = 118(3), P1–Pt1–H3 = 83.7(15), P1–Pt1–P2 = 102.19(7), P1–Pt1–N1 = 166.84(15), P2–Pt1–H3 = 172.7(15), P2–Pt1–N1 = 90.95(15), N1–Pt1–H3 = 83.3(15), Pt2–Pt1–P1 = 52.74(5), Pt2–Pt1–H3 = 30.9(15), Pt2–Pt1–P2 = 154.74(5), Pt2–Pt1–N1 = 114.19(15), P1–Pt2–H3 = 81.5(13), P1–Pt2–P3 = 157.96(7), P1–Pt2–P4 = 106.50(7), P3–Pt2–H3 = 77.5(13), P3–Pt2–P4 = 95.06(7), P4–Pt2–H3 = 170.5(12), Pt1–Pt2–P1 = 50.23(5), Pt1–Pt2–H3 = 31.2(12), Pt1–Pt2–P3 = 108.63(5), Pt1–Pt2–P4 = 156.10(5), H4···O1 = 2.44, P4–H4···O1 = 133, H1···F2i = 1.85, O1–H1···F2i = 2.647(7). Symmetry operator  $i = -x, y - 0.5, 0.5 - z$ .

distances was introduced, refinement of this density maximum, as the bridging H atom, converged with a physically meaningful displacement parameter and reasonable bond distances and angles.<sup>14</sup>

Complex  $[\text{2-CH}_3\text{CN}]^{2+}$  can be directly synthesized by treating an *n*-hexane/acetonitrile solution of **1** with  $\text{HBF}_4$  (either aqueous or etherate). The protonation to  $[\text{2-CH}_3\text{CN}]^{2+}$  is reversible: treating a  $\text{CHCl}_3$  solution of  $[\text{2-CH}_3\text{CN}]^{2+}$  with aqueous NaOH gives, first, the monocationic phosphinito complex  $[\text{3-CH}_3\text{CN}]^{+16}$  and eventually the starting compound **1** (Scheme 7).

The reaction of  $[\text{2-H}_2\text{O}]^{2+}$  with  $\text{PPh}_3$  in  $\text{CH}_2\text{Cl}_2$  gave quantitatively the substitution product  $[(\text{PHCy}_2)(\text{PPh}_3)\text{Pt}(\mu\text{-PCy}_2)(\mu\text{-H})\text{Pt}(\text{PHCy}_2)\{\kappa\text{-P-P(OH)Cy}_2\}]^{2+}(\text{Pt-Pt})$  ( $[\text{2-PPh}_3]^{2+}$ ; Scheme 8).

In the  $^{31}\text{P}\{^1\text{H}\}$  NMR spectrum of  $[\text{2-PPh}_3]^{2+}$ , the signal attributed to the bridging phosphanide was found at  $\delta$  171.9 as a

doublet of doublets due to the *trans* couplings with the coordinated  $\text{PPh}_3$  ( $^2J_{\text{P,P}} = 225$  Hz) and  $\text{P(OH)Cy}_2$  ( $^2J_{\text{P,P}} = 270$  Hz). The signal attributed to the coordinated  $\text{PPh}_3$  was found at  $\delta$  4.5 as a broad doublet ( $^2J_{\text{P,P}} = 225$  Hz), while the signals of the two coordinated  $\text{PHCy}_2$  ligands fell at  $\delta$   $-1.7$  ( $\text{P}^2$ ) and  $\delta$   $-3.1$  ( $\text{P}^4$ ). The two  $^{195}\text{Pt}$  NMR signals are almost isochronous, falling at  $\delta$   $-5705$  ( $\text{Pt}^1$ ) and  $\delta$   $-5684$  ( $\text{Pt}^2$ ).

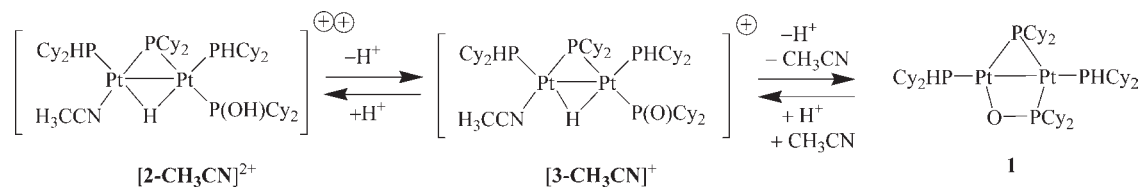
**Reaction with HF.** Hydrofluoric acid was chosen to investigate the protonation of **1** with a weak acid having a poorly coordinating anion.<sup>17</sup>

While no reaction occurred when an excess of  $\text{HF}_{(\text{aq})}$  was added to a toluene solution of **1**,<sup>18</sup> carrying out the reaction in dichloromethane led to dinuclear or tetranuclear Pt hydrides, depending on the experimental conditions.

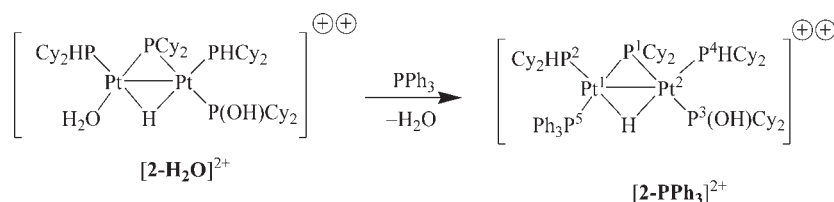
The addition of 2.5 equiv of concentrated hydrofluoric acid (50%<sub>w</sub>) to a dichloromethane solution of **1** gave the bis protonated complex  $[\text{2-H}_2\text{O}]^{2+}$ , whose counteranions were presumably the HF or  $\text{H}_2\text{O}$  adducts of fluoride,  $\{\text{F}(\text{HF})_n\}^-$  or  $\{\text{F}(\text{H}_2\text{O})_n\}^-$ , respectively.<sup>19</sup> For the sake of simplicity, in the following formulas, such counteranions will be denoted simply as  $\text{Y}^-$ . The species  $[\text{2-H}_2\text{O}](\text{Y})_2$  showed slightly different  $^1\text{H}$ ,  $^{31}\text{P}$ , and  $^{195}\text{Pt}$  NMR features compared to those of  $[\text{2-H}_2\text{O}][\text{BF}_4]_2$  (see the Experimental Section) presumably as a result of different interactions between the dication and the counteranions.<sup>20</sup> The formation of  $[\text{2-H}_2\text{O}]^{2+}$  by the protonation of **1** by  $\text{HF}_{(\text{aq})}$  indicates that when an excess of acid (HF or  $\text{HBF}_4$ ) is used, the reaction course is irrespective of the protonating agent, the counteranion of which serves only to neutralize the dicationic complex formed.

Complex  $[\text{2-H}_2\text{O}](\text{Y})_2$  was difficult to purify, as it consists of a mixture of several species differing for the counteranion (i.e.,  $\{\text{F}(\text{HF})\}^-$ ,  $\{\text{F}(\text{H}_2\text{O})\}^-$ ,  $\{\text{F}(\text{HF})_2\}^-$ , etc.). In solution,  $[\text{2-H}_2\text{O}](\text{Y})_2$  was found to transform spontaneously into the complex  $[(\text{PHCy}_2)\text{Pt}^1(\mu\text{-PCy}_2)\{\kappa^2\text{P}_2\text{O-}\mu\text{-P(O)Cy}_2\}\text{Pt}^2(\text{PHCy}_2)(\text{H})](\text{Y})(\text{Pt-Pt})$  (**6**)( $\text{Y}$ ), Scheme 9), the structure of which was inferred from its NMR features. The  $^1\text{H}$  NMR spectrum of **6**<sup>+</sup> showed a high-field signal at  $\delta$   $-1.61$  which was assigned, by means of  $^1\text{H}$ – $^{195}\text{Pt}$  HMQC experiments, to a terminal hydride directly bonded to  $\text{Pt}^2$  ( $^1J_{\text{H,Pt}(2)} = 832$  Hz). Such a signal appears as a dddd because of scalar couplings with four P atoms ( $J_{\text{H,P}} = 105$  Hz, 19 Hz, 16 Hz, 8 Hz). The  $^{31}\text{P}\{^1\text{H}\}$  NMR spectrum of **6**<sup>+</sup> showed four signals centered at  $\delta$  182.0,  $\delta$  80.6,  $\delta$  9.4, and  $\delta$   $-5.7$ . Of these, that at  $\delta$  182.0 splits into a doublet ( $J_{\text{P,H}} = 105$  Hz) in the proton coupled  $^{31}\text{P}$  NMR spectrum and was assigned to the bridging phosphanide subtending a Pt–Pt bond having the terminal hydride in the *trans* position. The signal at  $\delta$  80.6 was assigned to the bridging phosphinite bonded to  $\text{Pt}^1$  through the O atom and bonded to  $\text{Pt}^2$  through the P atom having in the *trans* position a dicyclohexylphosphane ( $\delta$   $-5.7$ ,  $^2J_{\text{P}(3),\text{P}(4)} = 157$

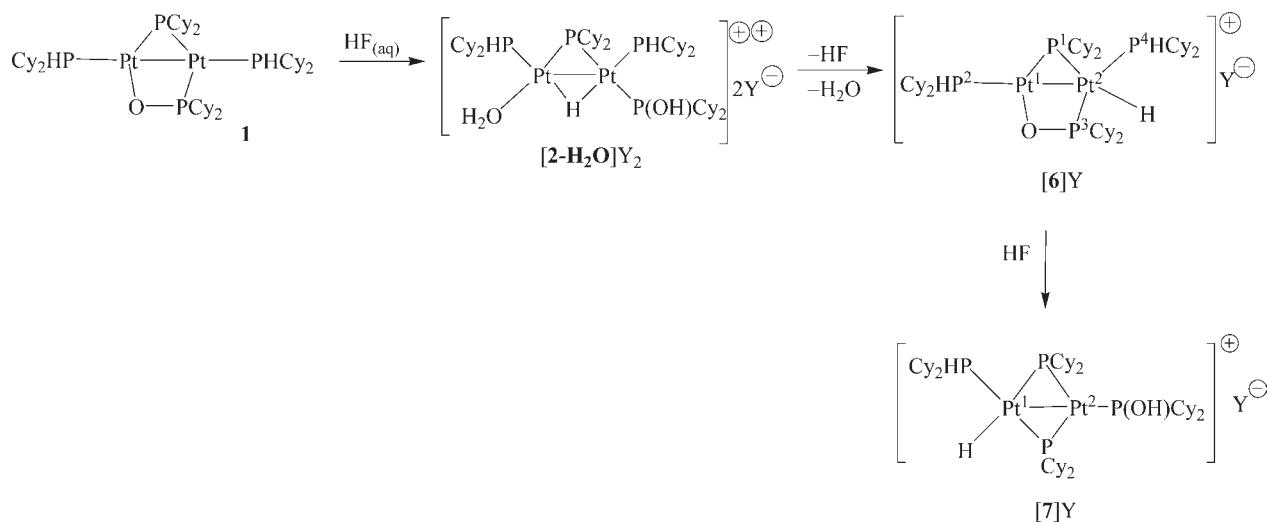
Scheme 7



Scheme 8



Scheme 9. Reaction of 1 with Concentrated Hydrofluoric Acid



Hz). The signal at  $\delta$  9.4 belongs to the  $P^2$  dicyclohexylphosphane bonded to  $Pt^1$  in the *trans* position with respect to the  $Pt^2$ . The  $^{195}Pt$  signals were found at  $\delta$  -5147 ( $Pt^1$ ) and  $\delta$  -5983 ( $Pt^2$ ).

The transformation of  $[2-H_2O](Y)_2$  into  $[6](Y)$ , never observed with  $[2-H_2O][BF_4]_2$ , points out a crucial role played by the fluoride-based  $Y^-$  counteranion, as confirmed by the almost complete transformation of  $[2-H_2O]^{2+}$  into  $[6]^+$  observed when a  $[2-H_2O][BF_4]_2$  was treated with a saturated aqueous solution of NaF at room temperature. Further details on the reaction pathway from  $[2-H_2O]^{2+}$  to  $[6]^+$  were obtained by DFT calculations and are reported below.

Monitoring by  $^{31}P$  NMR spectroscopy the solutions containing complex  $[6](Y)$  (plus residual  $[2-H_2O](Y)_2$  and HF) showed the transformation of  $[6](Y)$  into the bis-phosphanido-bridged Pt(II) dinuclear complex  $[(PHtBu_2)(H)Pt^1(\mu-PCy_2)_2-Pt^2\{P(OH)Cy_2\}](Y)(Pt-Pt)$  ( $[7](Y)$ , Scheme 9). The complex  $[7]^+$  is a dinuclear species containing two bridging phosphanides subtending a Pt-Pt bond according to their low field  $^{31}P$  NMR resonances<sup>21</sup> ( $\delta$  299.6 and  $\delta$  294.3). One Pt atom is tetracoordinated,

bearing, besides the bridging phosphanides, a terminal  $PHCy_2$  ( $\delta_P$  1.7) and a terminal hydride ( $\delta_H$  -2.84,  $^1J_{H,Pt(1)}$  833 Hz); the other Pt atom is tricoordinated, the ligand other than bridging phosphanides being a P-bound dicyclohexylphosphinic acid ( $\delta_P$  134.8). The structure of  $[7]^+$  is similar to that of the cationic complex  $[(PHtBu_2)(H)Pt(\mu-PtBu_2)_2Pt\{PHtBu_2\}]^+(Pt-Pt)$  obtained by the reaction of tetracyanoethylene with *anti*- $[(PHtBu_2)(H)Pt(\mu-PtBu_2)]_2$ .<sup>22</sup>

The transformation of a  $\mu$ -phosphanido/ $\mu$ -phosphinito complex into a bis  $\mu$ -phosphanido species has been already observed in the reaction of **1** with  $PHCy_2$ .<sup>3</sup> This suggests that, also in the present case, free  $PHCy_2$  formed upon dissociation from  $[6]^+$  may play a role in the isomerization  $[6]^+ \rightarrow [7]^+$ .

Finally, allowing a *diluted* (5%<sub>w</sub>) hydrofluoric acid solution to slowly diffuse in a dichloromethane solution of **1** at rt resulted in the formation, besides the species containing the Pt-Pt bond discussed above, of a new compound showing a distinctive  $^{31}P$  NMR multiplet centered at  $\delta$  -111.5, typical for bridging phosphanides *not* subtending a Pt-Pt bond,<sup>21</sup> a broad singlet at  $\delta$  6.0

## Scheme 10. Reactions of 1 with Aqueous HF under Conditions of Slow Diffusion of the Acid

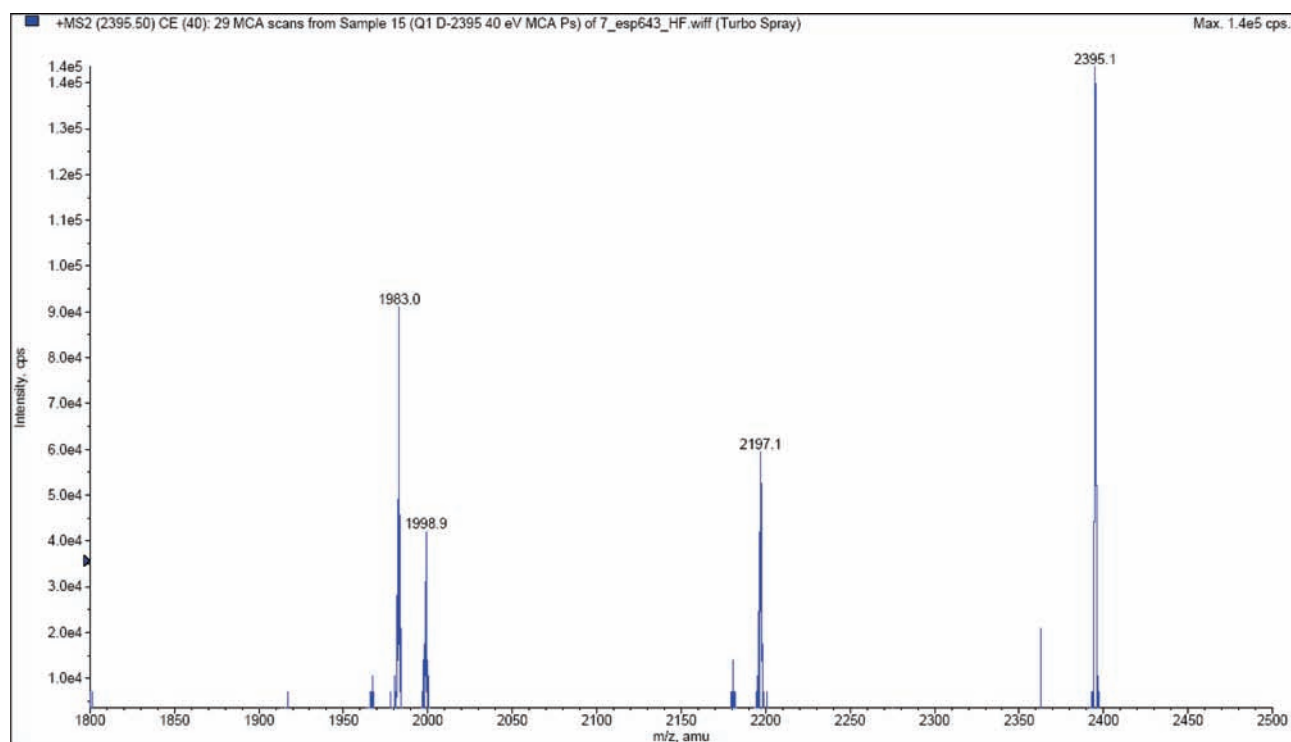
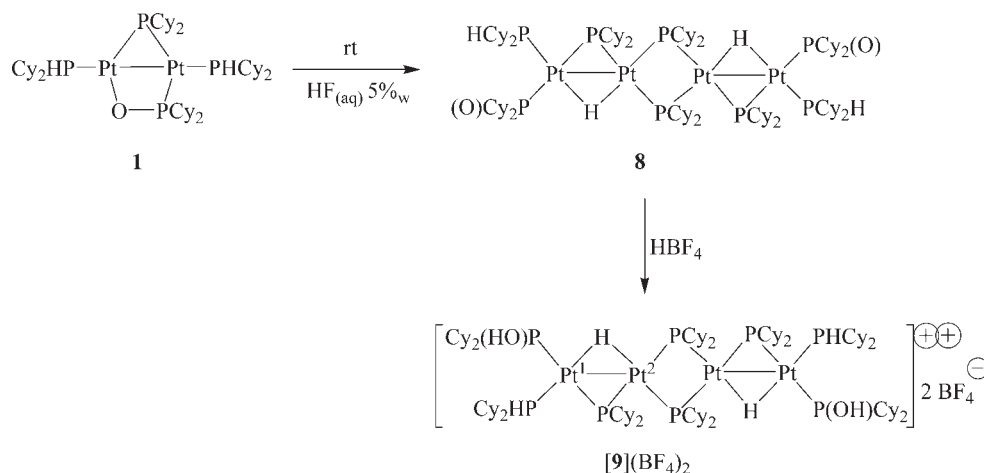


Figure 4. MS/MS spectrogram of 8 showing the fragmentation pattern of the ion at  $m/z$  2395.1.

ascrivable to a coordinated PHCy<sub>2</sub>, plus signals in the regions of coordinated P(O)Cy<sub>2</sub> ( $\delta$  ca. 80) and of bridging phosphanides subtending a Pt–Pt bond ( $\delta$  ca.138). Workup of the reaction mixture allowed us to isolate a white compound (8), which was found insoluble in solvents such as halogenated hydrocarbons, aromatic compounds, and dmso. Its IR spectrum in KBr showed a 1636 cm<sup>-1</sup> band ascribable to a bridging hydride and a single PH band at 2327 cm<sup>-1</sup>, while no bands typical for the POH moiety were present.

The structure proposed for 8 is reported in Scheme 10 and was confirmed by ESI-MS analysis and by its reactivity toward HBF<sub>4</sub>. The ESI-MS spectrogram of a very diluted chloroform solution of 8 showed the peaks at  $m/z$  2395.1, whose isotope pattern is

perfectly superimposable on that calculated for the ion [C<sub>96</sub>H<sub>181</sub>O<sub>2</sub>P<sub>8</sub>Pt<sub>4</sub>]<sup>+</sup> (corresponding to [8+H]<sup>+</sup>), and at  $m/z$  1198.1 ascribable to the doubly charged ion [8+2H]<sup>2+</sup>. The peak at  $m/z$  2395.1 was isolated for a MS/MS analysis, which showed a fragmentation pattern (Figure 4) consisting of the loss of a PHCy<sub>2</sub> ( $m/z$  = 2197.1), a P(OH)Cy<sub>2</sub> ( $m/z$  = 2181.0), two PHCy<sub>2</sub>'s ( $m/z$  = 1998.9), a PHCy<sub>2</sub>, and a P(OH)Cy<sub>2</sub> ( $m/z$  = 1983.0). All ions deriving from the fragmentation of [8+H]<sup>+</sup> were also observed (with their characteristic isotope pattern) in the ESI-MS spectrogram of 8.

The addition of HBF<sub>4</sub>·2Me<sub>2</sub>O to a suspension of 8 in CD<sub>2</sub>Cl<sub>2</sub> resulted in a pale yellow homogeneous solution of the

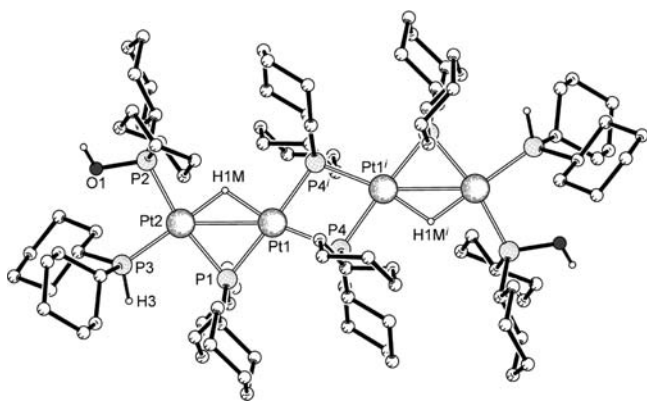


**Figure 5.** PLATON<sup>15</sup> drawing of  $[9]^{2+}$ . Hydrogen atoms bonded to C have been omitted for clarity. Interatomic distances (Å) and angles (deg): Pt(1)–P(1) 2.2883(19), Pt(1)–P(4) 2.3114(17), Pt(1)–P(4)i 2.3448(19), Pt(1)–Pt(2) 2.8994(6), Pt(1)–Pt(1)i 3.6539(11), Pt(1)–H(1M) 1.81(7), Pt(2)–P(3) 2.2684(19), Pt(2)–P(1) 2.3047(17), Pt(2)–P(2) 2.3079(18), Pt(2)–H(1M) 1.75(8), P(2)–O(1) 1.612(5), P(3)–H(3) 1.19(6), P(4)–Pt(1)i 2.3446(19); P(1)–Pt(1)–P(4) 108.04(6), P(1)–Pt(1)–P(4)i 167.07(6), P(4)–Pt(1)–P(4)i 76.61(6), P(1)–Pt(1)–Pt(2) 51.11(4), P(4)–Pt(1)–Pt(2) 157.33(5), P(4)i–Pt(1)–Pt(2) 125.78(4), P(1)–Pt(1)–H(1M) 85(2), P(4)–Pt(1)–H(1M) 166(2), P(4)i–Pt(1)–H(1M), 91(2), Pt(2)–Pt(1)–H(1M) 35(2), P(3)–Pt(2)–P(1) 94.71(6), P(3)–Pt(2)–P(2) 96.48(6), P(1)–Pt(2)–P(2) 167.02(6), P(3)–Pt(2)–Pt(1) 145.04(4), P(1)–Pt(2)–Pt(1) 50.61(5), P(2)–Pt(2)–Pt(1) 117.51(5), P(3)–Pt(2)–H(1M) 178(2), P(1)–Pt(2)–H(1M) 86(2), P(2)–Pt(2)–H(1M) 83(2), Pt(1)–Pt(2)–H(1M) 36(2), Pt(1)–P(1)–Pt(2) 78.29(5), O(1)–P(2)–Pt(2) 108.45(18), Pt(2)–P(3)–H(3) 113(3), Pt(1)–P(4)–Pt(1)i 103.39(6). Symmetry operator  $i = 1 - x, -y, 2 - z$ .

tetranuclear complex  $[(\text{P}(\text{H}(\text{C}_6\text{H}_{11})_2)\{\kappa\text{P}-\text{P}(\text{OH})\text{C}_6\text{H}_{11}\})\text{Pt}^i(\mu\text{-PCy}_2)(\mu\text{-H})\text{Pt}^j(\mu\text{-PCy}_2)]_2(\text{BF}_4)_2(\text{Pt}^i-\text{Pt}^j)$  ( $[9][\text{BF}_4]_2$ ).<sup>23</sup>

Also, the compound  $[9][\text{BF}_4]_2$ , once formed, tends to precipitate from dichloromethane but, differently from **8**, is soluble in  $\text{dms}-d_6$ . The  $^{31}\text{P}\{^1\text{H}\}$  NMR of complex  $[9]^{2+}$  in  $\text{dms}-d_6$  shows four signals at  $\delta$  138.1, 119.5, 0.6, and  $-111.1$ , all flanked by  $^{195}\text{Pt}$  satellites, attributable to the four pairs of nonequivalent P nuclei. The P atoms of the bridging phosphanides are involved in a second order spin system which was fully resolved by computer simulation (Figure S15, Supporting Information). The multiplets at  $\delta$  138.1 and  $\delta$   $-111.1$  are attributable to the bridging phosphanides subtending ( $\delta$  138.1) or not subtending ( $\delta$   $-111.1$ ) a Pt–Pt bond. The signal at  $\delta$  119.5 is a doublet of doublets due to couplings with the *trans* ( $^2J_{\text{P,P}} = 244$  Hz) and the *cis* ( $^2J_{\text{P,P}} = 25$  Hz) P atoms, attributable to the coordinated  $\text{P}(\text{OH})\text{C}_6\text{H}_{11}$ ; that at  $\delta$  0.6 is broad and falls in the region of the coordinated  $\text{PHC}_6\text{H}_{11}$ . The proton coupled  $^{31}\text{P}$  NMR spectrum confirms these attributions, as the only signal that significantly splits by passing from decoupled to coupled experiments is that at  $\delta$  0.6 ( $^1J_{\text{P,H}} = 355$  Hz). The  $^1\text{H}$  NMR spectrum shows, besides the signals due to cyclohexyl protons, (i) a deshielded singlet at  $\delta$  10.04 flanked by  $^{195}\text{Pt}$  satellites ( $^3J_{\text{H,Pt}} = 57$  Hz) attributable to the POH protons, (ii) a broad doublet at  $\delta$  5.28 flanked by  $^{195}\text{Pt}$  satellites ( $^2J_{\text{H,Pt}} = 65$  Hz) attributable to the H directly bonded to P ( $^1J_{\text{P,H}} = 355$  Hz), and (iii) a broad multiplet flanked by  $^{195}\text{Pt}$  satellites ( $^1J_{\text{H,Pt}(1)} = 576$  Hz,  $^1J_{\text{H,Pt}(2)} = 440$  Hz) centered at  $\delta$   $-5.85$ , attributable to the bridging hydrides. The NMR resonances of  $^{195}\text{Pt}^1$  and  $^{195}\text{Pt}^2$  were found at  $\delta$   $-5014$  and  $\delta$   $-5630$ , respectively.

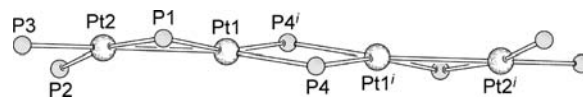
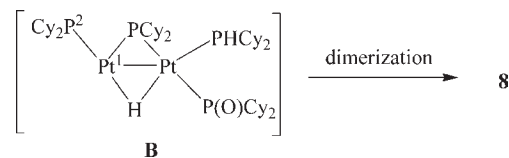


**Figure 6.** Skeleton of  $[9]^{2+}$ .

### Scheme 11



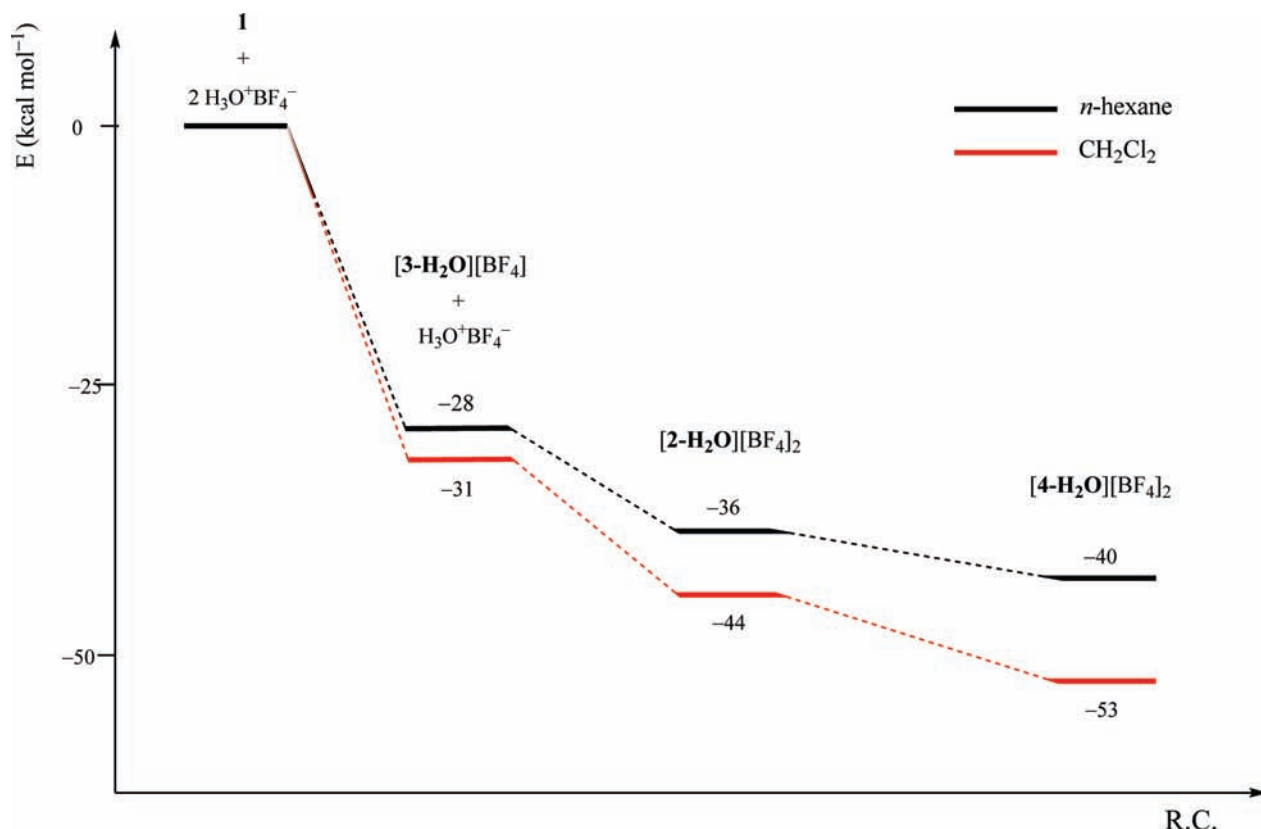
Crystals of  $[9][\text{BF}_4]_2$  suitable for X-ray analysis were obtained as a dichloromethane solvate from the slow evaporation of a  $\text{CH}_2\text{Cl}_2$  solution. The XRD structure of  $[9][\text{BF}_4]_2 \cdot 2\text{CH}_2\text{Cl}_2$  is shown in Figure 5. The compound consists of a divalent cationic complex, two  $\text{BF}_4^-$  ions, and two clathrated molecules of  $\text{CH}_2\text{Cl}_2$ .<sup>24</sup> The cation is a centrosymmetric tetrametallic complex in which the Pt atoms are bridged by four dicyclohexylphosphanido and two hydrido ligands. The structure can be regarded as two  $(\text{C}_6\text{H}_{11}\text{P})\{\kappa\text{P}-\text{PCy}_2(\text{OH})\}\text{Pt}(\mu\text{-PCy}_2)(\mu\text{-H})\text{Pt}^i$  subunits held together by two  $\text{PCy}_2$  groups to form a  $\text{Pt}_2\text{P}_2$  rhombus. The Pt1–Pt1' distance within this core is 3.6539(11) Å, indicating that there is no metal–metal bond. The intermetallic distance between the two Pt atoms of each subunit (Pt1–Pt2) is 2.8994(6) Å, in full agreement with the presence of a Pt–Pt bond. The different interatomic separations observed passing from Pt1–Pt1' to Pt1–Pt2 is reflected by the very different Pt– $\mu\text{P}$ –Pt angles which pass from 103.39(6)° (Pt1–P4–Pt1i) to 78.29(5)° (Pt1–P1–Pt2), a further confirmation of the renowned flexibility of bridging phosphanides.<sup>21</sup> The valence electron count for  $[9]^{2+}$  is 60, so the entire cation requires two metal–metal bonds to guarantee coordinative saturation to all Pt atoms, as found in the crystal structure. The coordination environments around the four Pt centers are essentially coplanar, as shown in Figure 6. The coordination planes of Pt2 and Pt1 subtend a dihedral angle of 15.0(16)°, whereas the ligands around Pt1 and Pt1' are coplanar for symmetry reasons. The  $\text{P}(\text{OH})\text{C}_6\text{H}_{11}$  hydrogen forms a hydrogen bond with the tetrafluoroborate anion, analogously to what was found for  $[2\text{-CH}_3\text{CN}][\text{BF}_4]_2$ . In the case of  $[9]^{2+}$ , the distance  $\text{F}_3\text{BF}_4 \cdots \text{HOP}$  is 2.02 Å and the  $\text{O}-\text{H} \cdots \text{F}$  angle is 157°.

Tetranuclear phosphanido complexes of Pt are rare. The known examples comprise cyclic complexes (featuring  $\text{Pt}_4\text{P}_4$ <sup>25</sup> or  $\text{Pt}_4\text{P}_2\text{I}_2$ <sup>26</sup> rings) as well as linear<sup>26,27</sup> and bent<sup>27b,28</sup> species.

The formation of **8** can be envisioned as deriving from the dimerization of fragment **B** (Scheme 11), which, in turn, can be supposed to form via deprotonation of the coordinated  $\text{P}^2\text{HCy}_2$  by the fluoride bases present in the environment, under the particular conditions employed for the synthesis.

**DFT Studies.** Density functional calculations were performed to study the energetics and the mechanism of the protonation reaction of **1** by  $\text{HBF}_4$  and  $\text{HF}$ . This study was carried out using models with methyl groups in place of cyclohexyl groups. The reliability of this model in reproducing the experimental geometrical parameters had already been proven for complexes **1**<sup>2</sup> and its protonation products with  $\text{HX}$  ( $\text{X} = \text{Cl}, \text{Br}$ )<sup>3</sup> and was confirmed for  $[2\text{-CH}_3\text{CN}][\text{BF}_4]_2$  and  $[9][\text{BF}_4]_2$ , the products of protonation



Scheme 12. Energy Diagram for the Stable Products of the Protonation Reaction of **1** with  $\text{H}_3\text{O}^+\text{BF}_4^-$ 

structurally characterized by XRD analysis, for which the calculated bond lengths and angles differ less than 0.06 Å and 5° from the experimental data. For the sake of simplicity, in the following discussion, we will not distinguish between the actual cyclohexyl-substituted complexes and their methyl-substituted models. The DFT calculations on [2-CH<sub>3</sub>CN][BF<sub>4</sub>]<sub>2</sub> and [9][BF<sub>4</sub>]<sub>2</sub> were performed considering explicitly the complexes as ion pairs, made up of a dinuclear or tetranuclear dicationic core and two BF<sub>4</sub><sup>-</sup> anions, as indicated by X-ray diffraction studies.

#### Reaction with HBF<sub>4</sub>

**Thermodynamics of the Formation of [3-L][BF<sub>4</sub>], [2-L][BF<sub>4</sub>]<sub>2</sub>, and [4-H<sub>2</sub>O][BF<sub>4</sub>]<sub>2</sub>.** We first addressed the thermodynamics of the protonation reaction of **1** with 1 or 2 equiv of HBF<sub>4</sub>, trying to account for all of the considered experimental conditions, i.e., the addition of aqueous HBF<sub>4</sub> to an *n*-hexane or dichloromethane solution of **1**, and the addition of etherate HBF<sub>4</sub> to the solution of **1** in acetone-*d*<sub>6</sub>, CD<sub>2</sub>Cl<sub>2</sub>, and acetonitrile. To this purpose, we considered the formation of the initial monoprotonated products, the [(PHCY<sub>2</sub>)(L)Pt(μ-PCY<sub>2</sub>)(μ-H)Pt{κP-P(O)CY<sub>2</sub>}(PHCY<sub>2</sub>)}(BF<sub>4</sub>) ion pairs, [3-L][BF<sub>4</sub>], and the final [(PHCY<sub>2</sub>)(L)Pt(μ-PCY<sub>2</sub>)(μ-H)Pt{κP-P(OH)CY<sub>2</sub>}(PHCY<sub>2</sub>)}(BF<sub>4</sub>)<sub>2</sub> products [2-L][BF<sub>4</sub>]<sub>2</sub>, with L = H<sub>2</sub>O, acetone-*d*<sub>6</sub>, CD<sub>2</sub>Cl<sub>2</sub>, and acetonitrile. According to the experimental procedure, the solvation effects were calculated for the solvent L itself when L = acetone-*d*<sub>6</sub>, CD<sub>2</sub>Cl<sub>2</sub>, and acetonitrile, and for both *n*-hexane and dichloromethane when L = H<sub>2</sub>O.

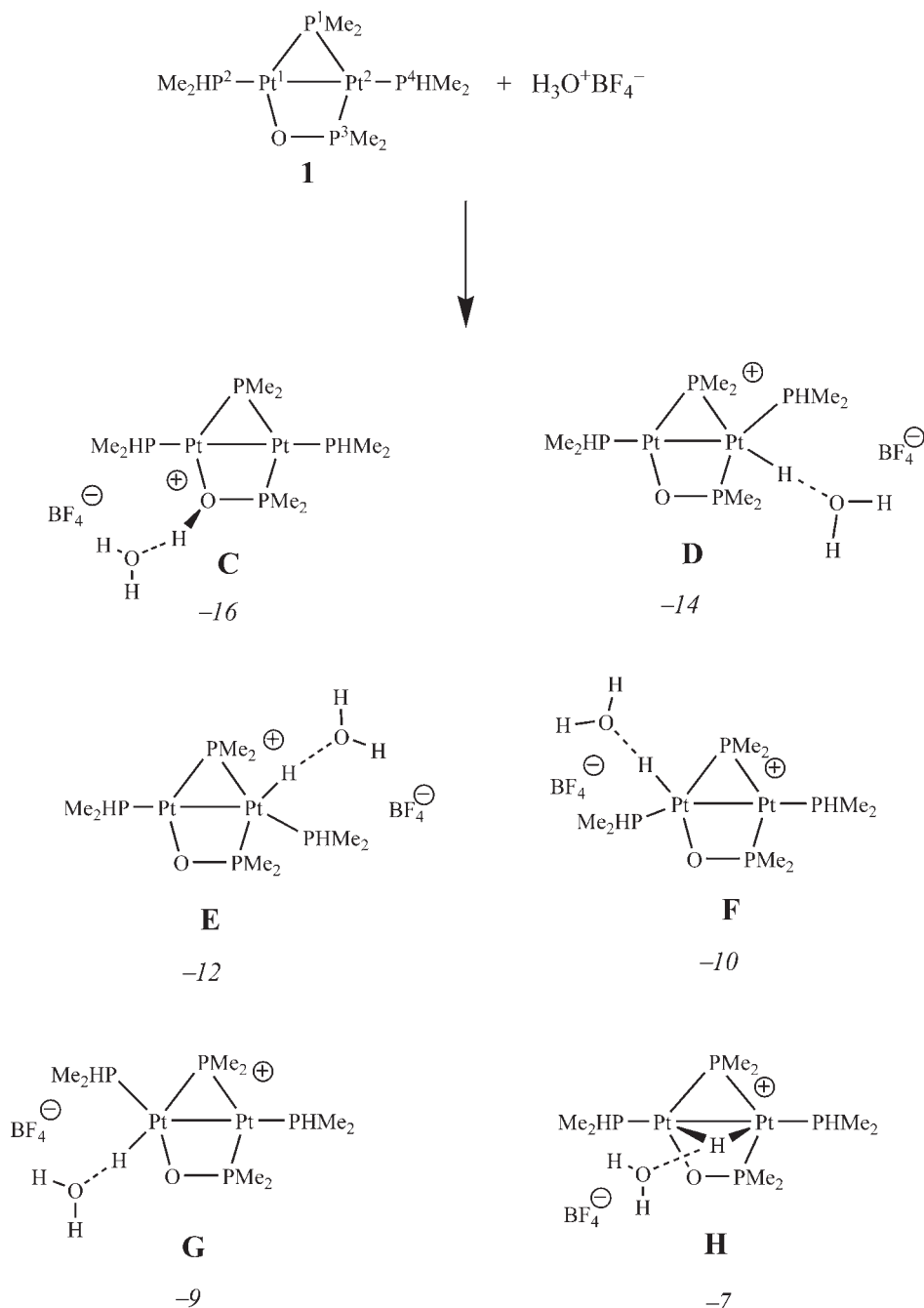
Special care was paid to consider the formation of [3-H<sub>2</sub>O][BF<sub>4</sub>] and [2-H<sub>2</sub>O][BF<sub>4</sub>]<sub>2</sub> from the addition of aqueous HBF<sub>4</sub> to an *n*-hexane or dichloromethane solution of **1**. Taking into account that HBF<sub>4</sub> is known to be completely ionized in aqueous

solutions,<sup>29</sup> as confirmed by our DFT calculations, indicating that the H<sub>3</sub>O<sup>+</sup>BF<sub>4</sub><sup>-</sup> ion pair is more stable than H<sub>2</sub>O and HBF<sub>4</sub> (by 8.8 kcal mol<sup>-1</sup> in *n*-hexane and 7.6 kcal mol<sup>-1</sup> in dichloromethane), we considered the H<sub>3</sub>O<sup>+</sup>BF<sub>4</sub><sup>-</sup> ion pair as the actual reacting species.

Scheme 12 shows an energy gain of 28 kcal mol<sup>-1</sup> in *n*-hexane (31 kcal mol<sup>-1</sup> in dichloromethane) for the protonation of **1** by 1 equiv of H<sub>3</sub>O<sup>+</sup>BF<sub>4</sub><sup>-</sup> leading to [3-H<sub>2</sub>O][BF<sub>4</sub>] and of a further 8 kcal mol<sup>-1</sup> (13 kcal mol<sup>-1</sup> in dichloromethane) for protonation by a second equivalent of H<sub>3</sub>O<sup>+</sup>BF<sub>4</sub><sup>-</sup>, leading to [2-H<sub>2</sub>O][BF<sub>4</sub>]<sub>2</sub>, with an overall reaction energy of -36 kcal mol<sup>-1</sup> (-44 kcal mol<sup>-1</sup> in dichloromethane) for the double protonation of **1**. Slightly higher values were calculated for the formation energies of [2-CD<sub>2</sub>Cl<sub>2</sub>][BF<sub>4</sub>]<sub>2</sub> (-48 kcal mol<sup>-1</sup>), [2-acetone-*d*<sub>6</sub>][BF<sub>4</sub>]<sub>2</sub> (-59 kcal mol<sup>-1</sup>), and [2-CH<sub>3</sub>CN][BF<sub>4</sub>]<sub>2</sub> (-65 kcal mol<sup>-1</sup>) from **1** and two HBF<sub>4</sub>'s plus one L solvent molecule. The corresponding energies for the formation of the corresponding [3-L][BF<sub>4</sub>] monoprotonated species are -27 kcal mol<sup>-1</sup> (L = CD<sub>2</sub>Cl<sub>2</sub>), -35 kcal mol<sup>-1</sup> (L = acetone), and -41 kcal mol<sup>-1</sup> (L = CH<sub>3</sub>CN).

Finally, we addressed the thermodynamics of the isomerization product [4-H<sub>2</sub>O][BF<sub>4</sub>]<sub>2</sub>, obtained when [2-H<sub>2</sub>O][BF<sub>4</sub>]<sub>2</sub> was left in a solution of halogenated solvents. Calculations indicated that the isomerization of [2-H<sub>2</sub>O]<sup>2+</sup> into [4-H<sub>2</sub>O]<sup>2+</sup> is an energetically favored process, even though by only 4 kcal mol<sup>-1</sup> (9 kcal mol<sup>-1</sup> in dichloromethane).

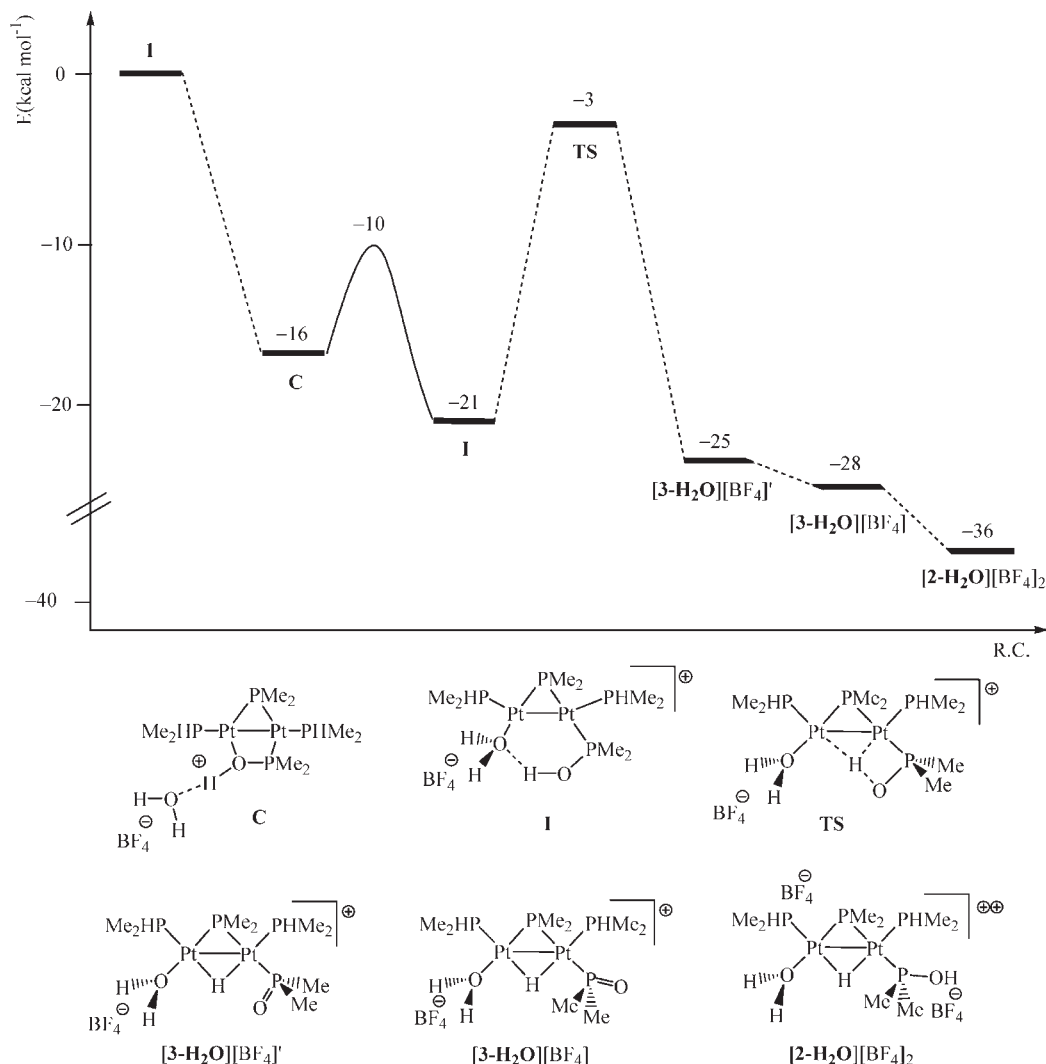
**Mechanism of Protonation.** Theoretical calculations were carried out to shed light on the mechanism of the protonation reaction of **1** with aqueous HBF<sub>4</sub>, calculating the energies of possible intermediates and the energy barriers of the main steps.

Scheme 13. Possible Ion Pairs for the Reaction of **1** with  $\text{H}_3\text{O}^+\text{BF}_4^-$ <sup>a</sup>

<sup>a</sup> Reaction energies are referred to **1** and the  $\text{H}_3\text{O}^+\text{BF}_4^-$  pair infinitely apart in *n*-hexane.

In principle, several potential protonation sites are available in complex **1**, that is, the two platinum atoms, the phosphinito oxygen, the metal–metal bond, and the Pt–P bonds. We first addressed the preliminary approach of the  $\text{H}_3\text{O}^+\text{BF}_4^-$  ion pair to **1** and investigated the formation of a hydrogen bond between the  $\text{H}_3\text{O}^+$  ion and each of these sites. Several geometry optimizations starting from various orientations of  $\text{H}_3\text{O}^+$  allowed us to locate five stable adducts corresponding to the formation of a hydrogen bond between  $\text{H}_3\text{O}^+$  and either the Pt<sup>1</sup> or Pt<sup>2</sup> atom (one of the three H–O bonds lying perpendicular to the platinum coordination plane), with two Pt–P bonds (one of the H–O bonds lying in the Pt<sup>1</sup> (Pt<sup>2</sup>) coordination plane and

interacting with both the bridging  $\mu\text{P}^1$  and the P<sup>2</sup> (P<sup>4</sup>) terminal phosphorus ligands), and with the Pt<sup>1</sup>–P<sup>2</sup> bond (the  $\text{H}_3\text{O}^+$  unit lying in the Pt<sup>1</sup> coordination plane *trans* to the bridging phosphinito ligand). The hydrogen bond adduct of the  $\text{H}_3\text{O}^+\text{BF}_4^-$  ion pair with the phosphinito oxygen undergoes a barrierless proton transfer leading to the dinuclear cationic species **C** (Scheme 13) in which a water molecule bridges the  $\text{BF}_4^-$  counteranion and the POH moiety. The species **C**, with a binding energy of 16 kcal mol<sup>-1</sup> with respect to **1** and  $\text{H}_3\text{O}^+\text{BF}_4^-$  infinitely apart, is by far more stable than the five calculated hydrogen bond adducts. Indeed, the adducts with a hydrogen bond between the  $\text{H}_3\text{O}^+\text{BF}_4^-$  pair and the Pt atoms

Scheme 14. Overall Energy Profile for the Reaction of **1** and the  $\text{H}_3\text{O}^+ \text{BF}_4^-$  Ion Pair Leading to  $[\text{2-H}_2\text{O}][\text{BF}_4]_2^a$ 

<sup>a</sup> Reaction energies are reported with respect to  $\mathbf{1} + \text{H}_3\text{O}^+\text{BF}_4^-$  or  $\mathbf{1} + 2\text{H}_3\text{O}^+\text{BF}_4^-$  in *n*-hexane.

showed bonding energies of 6–7 kcal mol<sup>-1</sup>, while the adducts where the interaction occurs with the Pt–P bonds showed bonding energies of 4–5 kcal mol<sup>-1</sup>.

We then studied the proton transfer process within each of the five calculated hydrogen-bonded adducts, performing geometry optimizations on the resulting H<sub>2</sub>O bridged ion pairs between the protonated dinuclear species and the BF<sub>4</sub><sup>-</sup> anion, and evaluating their energies with respect to **1** and H<sub>3</sub>O<sup>+</sup>BF<sub>4</sub><sup>-</sup> infinitely apart. All geometry optimizations led to five further minima on the potential energy surface for **1** plus H<sub>3</sub>O<sup>+</sup>BF<sub>4</sub><sup>-</sup> corresponding to the protonation of one platinum atom (**D**, **E**, **F**, and **G**) and to the metal–metal bond (**H**) (Scheme 13). The calculated energy gains for the corresponding ion pairs range from 7 to 14 kcal mol<sup>-1</sup>, showing bonding energies lower than that found for **C** (16 kcal mol<sup>-1</sup>).

These results indicate the oxygen protonated structure **C** as the most stable species formed by proton transfer from H<sub>3</sub>O<sup>+</sup>BF<sub>4</sub><sup>-</sup> to **1**. This behavior parallels what was found for the protonation of **1** with HCl and had already been rationalized in terms of the high negative charge on the O atom, the easier proton approach to O (less hampered by steric hindrance of the large cyclohexyl groups than the

Pt atoms), the high contribution of the p(O) orbital to the HOMO of **1**, and the formation of the complexes with the smallest structural changes relative to the parent species **1**.<sup>3</sup>

We then addressed the mechanism leading from the initially formed ion pair **C** to the final product  $[\text{2-H}_2\text{O}][\text{BF}_4]_2$ , trying to identify the main intermediates and transition states. As shown in Scheme 2, the protonation of **1** with strong hydrohalic acids HX (X = Cl, Br, I) passes through intermediates **A**, endowed with a six-membered Pt–X···H–O–P–Pt ring that evolves first into the monoprotonated compounds  $[(\text{PHCY}_2)(\text{X})\text{Pt}(\mu\text{-PCY}_2)(\mu\text{-H})\text{Pt}(\text{CY}_2\text{PH})\{\kappa\text{P-P}(\text{O})\text{CY}_2\}](\text{Pt-Pt})$  and then, in the presence of excess acid, into the diprotonated compounds,  $[(\text{PHCY}_2)(\text{X})\text{Pt}(\mu\text{-PCY}_2)(\mu\text{-H})\text{Pt}(\text{CY}_2\text{PH})\{\kappa\text{P-P}(\text{OH})\text{CY}_2\}]\text{X}(\text{Pt-Pt})$ . Although monitoring the protonation of **1** by VT-NMR with aqueous HBF<sub>4</sub> in *n*-hexane did not reveal any signal attributable to a six-membered platinumacycle intermediate **I** similar to **A** (with H<sub>2</sub>O in place of the Cl ligand), we have nonetheless assumed for the protonation by HBF<sub>4</sub>(aq) a path similar to that found for HCl, i.e., the sequence  $\mathbf{1} \rightarrow \mathbf{C} \rightarrow \mathbf{I} \rightarrow [\mathbf{3-H}_2\text{O}]^+$  (Scheme 14). Indeed, a geometry optimization led to a stable minimum for the putative intermediate **I** (see Figure 7), 5 kcal

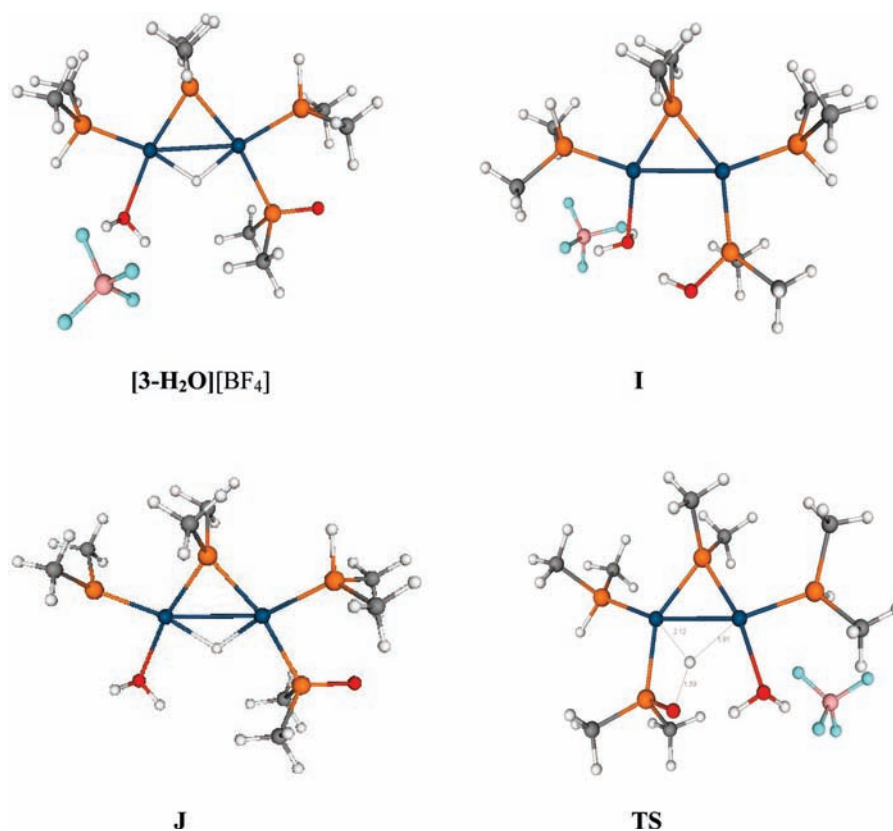


**Figure 7.** Structures of some intermediates and transition states of the protonation of **1** with aqueous  $\text{HBF}_4$  or  $\text{HF}$ , see text.

$\text{mol}^{-1}$  more stable than **C** and  $21 \text{ kcal mol}^{-1}$  than **1** and  $\text{H}_3\text{O}^+ \cdot \text{BF}_4^-$  infinitely apart.

Moreover, the significant elongation of the  $\text{Pt}^1\text{—O}$  bond upon oxygen protonation, from  $2.18 \text{ \AA}$  in **1** to  $2.32 \text{ \AA}$  in **C**, indicates a high degree of bond weakening and suggests a low-energy pathway for the migration of the  $\text{H}_2\text{O}$  hydrogen bonded to the phosphinic acid in the initially formed ion pair **C** to the  $\text{Pt}^1$  left coordinatively unsaturated by the detachment of the oxygen and leading to the six-membered intermediate **I**.

This point was further investigated by calculating the energy profile for this pathway, taking the  $\text{Pt—O}(\text{water})$  distance as a reaction coordinate. This distance was varied from  $4.19 \text{ \AA}$ , the value in **C**, to  $2.32 \text{ \AA}$ , the value in **I**, optimizing all of the remaining geometrical parameters at each fixed value of the reaction coordinate. The calculated energy profile (Scheme 14) indicates that this is a facile exothermic process, with a reaction energy of  $-5 \text{ kcal mol}^{-1}$  and a maximum of only  $6 \text{ kcal mol}^{-1}$ , suggesting that **C** is a highly unstable species which evolves immediately to **I**.

We then considered also the energy profile of the intramolecular rearrangement from **I** to the monoprotonated species  $[\text{3-H}_2\text{O}]^+$  (Scheme 14). In this case, the distance between the hydrogen bridging the oxygen atoms and the midpoint of the  $\text{Pt—Pt}$  bond was taken as the reaction coordinate, which was varied from  $3.35 \text{ \AA}$ , the value in **I**, to  $1.07 \text{ \AA}$ , the final value in  $[\text{3-H}_2\text{O}]^+$ , obtaining a maximum in the energy profile ca.  $21 \text{ kcal mol}^{-1}$  above **I**. Since the chosen reaction coordinate is only approximate, and the corresponding maximum is quite high, we performed a transition state search starting from the structure of the maximum. This procedure gave a structure for the **TS**  $18 \text{ kcal mol}^{-1}$  above that for **I** (Figure 7). The frequency analysis gave an

imaginary frequency of  $1228 \text{ cm}^{-1}$  corresponding to the expected normal mode. This transition state is actually connected to a conformer  $[\text{3-H}_2\text{O}]^{+ \prime}$ , having the phosphinito oxygen directed toward the bridging hydride, slightly less stable (by  $3 \text{ kcal mol}^{-1}$ ) than the global minimum  $[\text{3-H}_2\text{O}]^+$ , where the oxygen atom is directed away from the bridging hydride, and to which it is expected to easily relax. These results show that the proton transfer from the phosphinito oxygen to the  $\text{Pt—Pt}$  bond is an exothermic process (by  $7 \text{ kcal mol}^{-1}$ ) with a relatively low energy barrier,  $18 \text{ kcal mol}^{-1}$ , indicating that the intramolecular conversion of **I** into  $[\text{3-H}_2\text{O}]^+$  is a quite facile process. The difference between the energy barrier found for the analogous process operative during the protonation of **1** by  $\text{HCl}$  ( $29$  vs  $18 \text{ kcal mol}^{-1}$ ) may be held responsible for the fact that the intermediate **I** was undetectable by NMR spectroscopy even at low  $T$ .

The lower energy barrier for the proton transfer from the oxygen to the  $\text{Pt—Pt}$  bond observed for the  $\text{I} \rightarrow [\text{3-H}_2\text{O}]^+$  transformation with respect to the  $\text{A} \rightarrow [\text{3-Cl}]$  one could be due to the slightly higher electron charge on the  $\text{Pt—Pt}$  bond present in the former case.

We also addressed the second protonation step of **1**, i.e., the protonation of  $[\text{3-H}_2\text{O}][\text{BF}_4^-]$  by  $\text{H}_3\text{O}^+ \cdot \text{BF}_4^-$  to give  $[\text{2-H}_2\text{O}][\text{BF}_4^-]_2$ . In principle, the protonation sites in  $[\text{3-H}_2\text{O}]^+$  are represented by the platinum atoms, the bridging hydride, the  $\text{Pt—P}$  bonds, the aqua ligand, and the phosphinito oxygen. By considering the interaction of  $[\text{3-H}_2\text{O}]^+$  with a  $\text{H}_3\text{O}^+ \cdot \text{BF}_4^-$  ion pair, we looked for the possible hydrogen-bonded adducts by energy optimization of several starting geometries with all possible orientations of the attacking  $\text{H}_3\text{O}^+$  unit. Stable hydrogen-bound adducts were found for the  $\text{H}_3\text{O}^+$  moiety interacting

with the Pt atoms, the Pt–P bonds, and the aqua ligand, with bonding energies in the range of 2–10 kcal mol<sup>-1</sup>. However, the hydrogen bond adduct of H<sub>3</sub>O<sup>+</sup>BF<sub>4</sub><sup>-</sup> with the phosphinito oxygen undergoes a barrierless proton transfer leading to the final product [2-H<sub>2</sub>O][BF<sub>4</sub>]<sub>2</sub> where the transferred proton on the oxygen atom interacts with the BF<sub>4</sub><sup>-</sup> anion through two hydrogen bonds with a bridging H<sub>2</sub>O molecule. Therefore, our calculations indicate that [3-H<sub>2</sub>O][BF<sub>4</sub>]<sup>-</sup> is spontaneously protonated by a H<sub>3</sub>O<sup>+</sup>BF<sub>4</sub><sup>-</sup> ion pair at the phosphinito oxygen, leading to [2-H<sub>2</sub>O][BF<sub>4</sub>]<sub>2</sub> with an energy gain of 8 kcal mol<sup>-1</sup> (Scheme 14).

#### Reaction with HF

**Thermodynamics and Mechanism of Protonation of 1 by HF.** We also considered the protonation reaction of **1** with HF, trying to shed light on the reasons for the different behavior shown by this acid compared to the other halohydric acids (HCl, HBr, and HI), on one hand, and on the analogies with the behavior of HBF<sub>4</sub>, on the other hand. We thus addressed the thermodynamics of the protonation reaction of **1** with one HF molecule in dichloromethane and compared it with the thermodynamics, already investigated by us,<sup>3</sup> for the analogous reaction with HCl, HBr, and HI. The comparison indicates that while the protonation of **1** by 1 equiv of HX (X = Cl, Br, I) to [3-X] leads to an energy gain of 34–44 kcal mol<sup>-1</sup>, the protonation by HF to give the hypothetical product [3-F] leads to an energy gain of only 19 kcal mol<sup>-1</sup>. The reason for such a low formation energy calculated for [3-F] can be attributed to the well-known low affinity of Pt(II) for the F<sup>-</sup> ligand,<sup>30</sup> and ultimately to the low Pt–F bond energy. To further investigate this point, we calculated the energy required to detach the X<sup>-</sup> ion from the [3-X] species in a CH<sub>2</sub>Cl<sub>2</sub> solution, estimating Pt–X bond energies of 43–48 kcal mol<sup>-1</sup> for X = Cl, Br, and I and only 33 kcal mol<sup>-1</sup> for X = F. An analogous calculation on the detachment of the H<sub>2</sub>O molecule from [3-H<sub>2</sub>O]<sup>+</sup> leads to a Pt–OH<sub>2</sub> bond energy of 35 kcal mol<sup>-1</sup>, a value slightly higher than that of the Pt–F bond, but still much lower than those of the Pt–Cl, Pt–Br, and Pt–I bonds.

The relatively low value calculated for the formation energy of [3-F] (19 kcal mol<sup>-1</sup>) and the comparable bond energies found for the Pt–F and Pt–OH<sub>2</sub> bonds (33–35 kcal mol<sup>-1</sup>) give a rationale for the fact that neither [3-F] nor the corresponding doubly protonated [2-F]<sup>+</sup> species could be isolated from reactions of **1** with hydrofluoric acid.

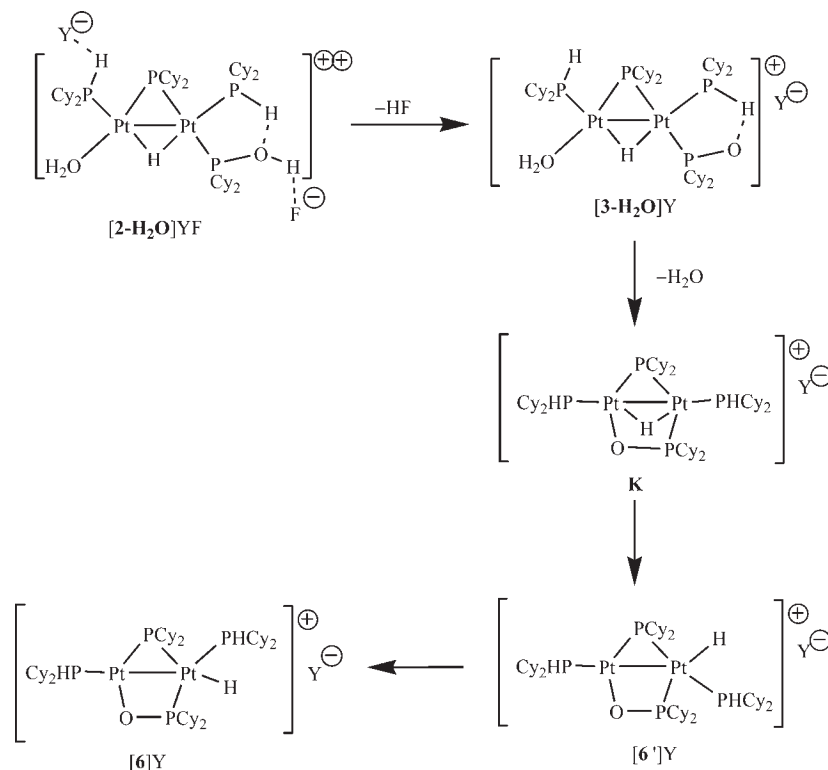
Unfortunately, an accurate calculation of the thermodynamics for the protonation of **1** by 1 and 2 equiv of HF leading to [3-H<sub>2</sub>O](Y) and [2-H<sub>2</sub>O](Y)<sub>2</sub>, respectively, was prevented by the subtle nature of the Y<sup>-</sup> counteranion, which is related to the complicated behavior of HF in aqueous solution. Indeed, several experimental and theoretical studies in recent decades have shown that an aqueous solution of hydrofluoric acids are made up of a complex mixture of hydrogen bonded HF/H<sub>2</sub>O clusters in equilibrium with tightly bound [H<sub>2</sub>O⋯H<sup>+</sup>⋯F<sup>-</sup>] ion pairs stabilized by hydrogen bonding with neighboring H<sub>2</sub>O and HF molecules; while at low concentrations these ion pairs are quite stable, at high HF concentrations they dissociate into H<sub>3</sub>O<sup>+</sup>, stabilized by hydrogen bonding with HF and H<sub>2</sub>O, and a variety of polyfluoride [F(HF)<sub>n</sub>]<sup>-</sup> and [F(HF)<sub>n</sub>(H<sub>2</sub>O)<sub>m</sub>]<sup>-</sup> anions with n + m varying from one to four.<sup>19</sup>

The results of geometry optimization for [3-H<sub>2</sub>O](Y) and [2-H<sub>2</sub>O](Y)<sub>2</sub> strongly depend on the kind of species which is actually employed to simulate the Y<sup>-</sup> counteranion in the calculations. In particular, when a bare F<sup>-</sup> ion was employed

and initially placed in the same positions occupied by the BF<sub>4</sub><sup>-</sup> ion in the X-ray structure of [2-CH<sub>3</sub>CN][BF<sub>4</sub>]<sub>2</sub>, i.e., close to and interacting with the hydrogen atoms of the phosphinic acid and of the P<sup>+</sup>HCy<sub>2</sub> ligands (see Figure 3), a barrierless proton transfer occurred from the phosphinito oxygen and even from the phosphane P atom to the F<sup>-</sup> ion, leading to one or two HF molecules and a neutral [(PCy<sub>2</sub>)(H<sub>2</sub>O)Pt(μ-PCy<sub>2</sub>)(μ-H)Pt-(PHCy<sub>2</sub>)<sub>2</sub>]{κP-P(O)Cy<sub>2</sub>}(Pt–Pt) species, **J** (corresponding to **B**, Scheme 11, but with Pt<sup>I</sup> bonded to H<sub>2</sub>O), featuring a terminal PCy<sub>2</sub><sup>-</sup> ligand (Figure 7). The proton transfer occurs even if the geometry optimization is carried out in a CH<sub>2</sub>Cl<sub>2</sub> solution, indicating that this is not an artifact of the gas-phase calculation. The same result was obtained when a [F(HF)]<sup>-</sup> ion was employed to simulate the Y<sup>-</sup> counteranion in the calculations, the proton transfer leading to the same neutral Pt–Pt species and to one or two (HF)<sub>2</sub> dimers. Only when a larger [F(HF)<sub>n</sub>]<sup>-</sup> (n = 2–4) counteranion was employed, with two to four HF molecules stabilizing the F<sup>-</sup> ion, did the geometry optimization lead to the expected [3-H<sub>2</sub>O](Y) ion pair and [2-H<sub>2</sub>O](Y)<sub>2</sub> ion triple complexes. Unfortunately, the large size of these anions, their floppiness, and the flatness of the potential energy surface for their interaction with the dinuclear [3-H<sub>2</sub>O]<sup>+</sup> or [2-H<sub>2</sub>O]<sup>2+</sup> cations led to convergence difficulties and exponentially increased the computational load, making extensive calculations on the thermodynamics and kinetics of the protonation of **1** by HF an extremely difficult task, out of the scope of this study.

Nonetheless, our calculations gave important indications on the protonation of **1** by HF:

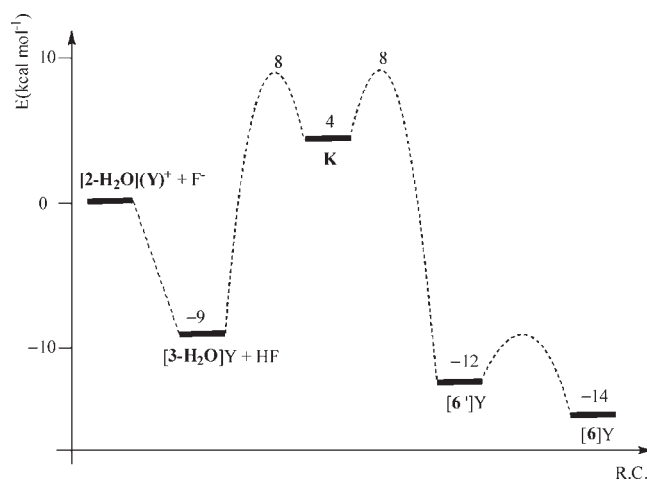
- (i) For Y<sup>-</sup> = [F(HF)<sub>n</sub>]<sup>-</sup> (n = 2–4), the calculated geometries for [3-H<sub>2</sub>O](Y) and [2-H<sub>2</sub>O](Y)<sub>2</sub> are very close to those calculated for [3-H<sub>2</sub>O][BF<sub>4</sub>]<sup>-</sup> and [2-H<sub>2</sub>O][BF<sub>4</sub>]<sub>2</sub>, in agreement with the NMR indications. This result also suggests that stable [3-H<sub>2</sub>O](Y) and [2-H<sub>2</sub>O](Y)<sub>2</sub> form only with oligomeric counteranions Y<sup>-</sup> where the F<sup>-</sup> ion is stabilized by tight hydrogen bonds with at least two HF molecules.
- (ii) For the [F(HF)<sub>2</sub>]<sup>-</sup> or [F(HF)<sub>3</sub>]<sup>-</sup> counteranions, presumably close to the actual ones, we could also calculate the formation energies of [3-H<sub>2</sub>O](Y) and [2-H<sub>2</sub>O](Y)<sub>2</sub> from **1** and one or two H<sub>3</sub>O<sup>+</sup>Y<sup>-</sup> ion pairs in a dichloromethane solution, obtaining values of 24 and 43 kcal mol<sup>-1</sup> (for Y<sup>-</sup> = [F(HF)<sub>2</sub>]<sup>-</sup>) and 25 and 41 kcal mol<sup>-1</sup> (for Y<sup>-</sup> = [F(HF)<sub>3</sub>]<sup>-</sup>), respectively. Such values are similar to those obtained for the formation of [3-H<sub>2</sub>O]-[BF<sub>4</sub>]<sup>-</sup> and [2-H<sub>2</sub>O][BF<sub>4</sub>]<sub>2</sub> from **1** and one or two H<sub>3</sub>O<sup>+</sup>(BF<sub>4</sub>)<sup>-</sup> ion pairs in the same solvent, see Scheme 12. Interestingly, if the formation energies of [3-H<sub>2</sub>O](Y) and [2-H<sub>2</sub>O](Y)<sub>2</sub> are calculated in toluene, much lower values are obtained (15 and 34 kcal mol<sup>-1</sup> for Y<sup>-</sup> = [F(HF)<sub>2</sub>]<sup>-</sup> and 16 and 33 kcal mol<sup>-1</sup> for Y<sup>-</sup> = [F(HF)<sub>3</sub>]<sup>-</sup>, respectively) which could partly account for the lack of reactivity of **1** with HF in this solvent.
- (iii) The results of the geometry optimization for [3-H<sub>2</sub>O](Y) and [2-H<sub>2</sub>O](Y)<sub>2</sub> when using, as a counteranion, F<sup>-</sup> bare or solvated by only one HF molecule indicate that these anions are sufficiently basic to abstract a proton from the phosphinito O and phosphane P atoms. These kinds of anions are expected to be present in diluted HF solutions or to form upon the addition of an excess of fluoride anions, conditions in which there are not enough HF molecules to form [F(HF)<sub>n</sub>]<sup>-</sup> (n = 2–4) species. When the protonation of **1** is carried out in diluted HF,

Scheme 15. Reaction Scheme for the Formation of [6](Y) from [2-H<sub>2</sub>O](Y)(F) (Y<sup>-</sup> = [F(HF)<sub>3</sub>]<sup>-</sup>)

the initially formed [3-H<sub>2</sub>O]<sup>+</sup> can be deprotonated to J, which is expected to easily dimerize to the tetranuclear species 8, in good agreement with the experimental findings.

Only the formation of [6]<sup>+</sup> and of 8 was addressed in detail. We first faced the formation of [6](Y) from [2-H<sub>2</sub>O](Y)(F) considering an F<sup>-</sup> anion approaching the phosphinito hydroxyl and a stable Y<sup>-</sup> = [F(HF)<sub>3</sub>]<sup>-</sup> anion hydrogen-bonded to a terminal phosphane hydrogen. The initial step, i.e., the proton abstraction from the phosphinito oxygen in [2-H<sub>2</sub>O](Y)(F) by the F<sup>-</sup> counteranion leading to [3-H<sub>2</sub>O](Y) and a HF moiety, is an exoenergetic and barrierless process, for which we calculated an energy gain of 9 kcal mol<sup>-1</sup>. The subsequent coordination of the phosphinito oxygen in [3-H<sub>2</sub>O](Y) to the Pt<sup>I</sup> atom leading to the formation of the final [6](Y) species is also exoenergetic by 5 kcal mol<sup>-1</sup> so that for the overall formation of [6](Y) from [2-H<sub>2</sub>O](Y)(F) we calculated a reaction energy of 14 kcal mol<sup>-1</sup>.

In order to study the kinetics of the isomerization of [3-H<sub>2</sub>O](Y) to [6](Y) and to shed light on its mechanism, we calculated the energy profile for the binding of the phosphinito oxygen to the Pt<sup>I</sup> atom in [3-H<sub>2</sub>O](Y) as the initial step for the formation of [6](Y). As the reaction coordinate was taken, the Pt–O distance was varied from 4.19 Å, the value in [3-H<sub>2</sub>O](Y), to 2.32 Å, the value in the final product [6](Y), optimizing all of the remaining geometrical parameters at each fixed value of this reaction coordinate. The calculated energy profile (Scheme 16) shows that the oxygen coordination to Pt<sup>I</sup> causes the detachment of the water molecule but not of the bridging hydrogen atom from Pt<sup>I</sup> and leads to the formation of a [(PHCy<sub>2</sub>)Pt(μ-PCy<sub>2</sub>)-(μ-H){κ<sup>2</sup>P,O-μ-P(O)Cy<sub>2</sub>}Pt(PHCy<sub>2</sub>)](Y)(Pt–Pt) species, K (Scheme 15), characterized by the simultaneous presence of a

Scheme 16. Energy profile for the formation of [6](Y) from [2-H<sub>2</sub>O](Y)(F) (Y<sup>-</sup> = [F(HF)<sub>3</sub>]<sup>-</sup>)

hydrogen and phosphinito bridges and indicates a relatively facile process, with a maximum—an upper limit to the energy barrier—of 17 kcal · mol<sup>-1</sup>. A second energy profile was then calculated for the rupture of the Pt<sup>I</sup>–H bond and formation of a terminal Pt<sup>2</sup>–H species, taking the Pt<sup>I</sup>–H distance as a reaction coordinate and varying it from 1.71 Å, the value in K, to 3.84 Å, the value in [6](Y). The results indicate the formation of the isomer [6'](Y) rather than [6](Y) and a barrier of only 4 kcal · mol<sup>-1</sup>, indicating that this is a very easy process. The isomer [6'](Y) is slightly less stable than [6](Y), by 2 kcal mol<sup>-1</sup>, to which it is expected to easily isomerize and which is therefore the final product of the

reaction. The overall process can therefore be considered to occur through the mechanism reported in Scheme 15.

Intrigued by this result, we have carried out the reaction of **1** with an 8-fold excess of hydrofluoric acid at 258 K in  $\text{CD}_2\text{Cl}_2$ , and we were pleased to find that, at this temperature and after 1 h, distinctive signals attributable to the isomer  $[\mathbf{6}'](\text{Y})^{31}$  together with those attributed to  $[\mathbf{2}\text{-H}_2\text{O}](\text{Y})_2$  appeared in  $^{31}\text{P}\{^1\text{H}\}$ ,  $^1\text{H}$ , and  $^{195}\text{Pt}\{^1\text{H}\}$  NMR spectra of the reaction mixture. As expected, warming the reaction mixture up to 298 K triggered the quantitative  $[\mathbf{6}'](\text{Y}) \rightarrow [\mathbf{6}](\text{Y})$  isomerization, as evidenced by NMR spectroscopy.

We finally evaluated the reaction energies for the steps involved in the formation of **8** from  $[\mathbf{3}\text{-H}_2\text{O}](\text{Y})$ , for  $\text{Y}^- = \text{F}^-$  interacting with the hydrogen atom on the phosphane coordinated to Pt<sup>I</sup>. The first step, corresponding to a proton abstraction from the P<sup>2</sup> phosphorus (i.e., the P *cis* to H<sub>2</sub>O) in  $[\mathbf{3}\text{-H}_2\text{O}](\text{F})$  by the F<sup>-</sup> counteranion leading to **J** and a HF moieties, is an exoenergetic and barrierless process, for which energy gains of 3 kcal mol<sup>-1</sup> were calculated. The subsequent dimerization of two **J** units, leading to the tetramer species **8**, is a thermodynamically favored process with a reaction energy of 15 kcal mol<sup>-1</sup> and is also expected to show a small energy barrier (not evaluated) corresponding to the detachment of the water molecule in **J**.

## CONCLUSIONS

Experimental and DFT data allowed us to outline the course of the protonation of the phosphinito-bridged Pt(I) complex **1** with HBF<sub>4</sub> or HF, which, in general, parallels that already described for halohydric acids such as HCl and HBr. In fact, hydrido-bridged dicyclohexylphosphinic acid Pt(II) dinuclear complexes  $[(\text{PHCY}_2)(\text{X})\text{Pt}(\mu\text{-PCY}_2)(\mu\text{-H})\text{Pt}(\text{PHCY}_2)\{\kappa\text{P-P}(\text{OH})\text{CY}_2\}]^{n+}(\text{Pt-Pt})$  ( $[\mathbf{2}\text{-X}]^{n+}$ , X = Cl, Br,  $n = 1$ ; X = H<sub>2</sub>O, acetone, dichloromethane, CH<sub>3</sub>CN,  $n = 2$ ) are formed in all cases with excess acid. However, in the case of HBF<sub>4</sub> or HF, the poorly coordinating anions of these Brønsted acids are not incorporated in the protonation products, which bear solvent molecules (H<sub>2</sub>O, acetone, dichloromethane, acetonitrile) in order to fulfill the coordination requirements of the platinum. Moreover, differently from the protonation products obtained with HCl or HBr, which are indefinitely stable in solution, the hydrido-bridged dicyclohexylphosphinic acid Pt(II) dinuclear complexes obtained with HBF<sub>4</sub> or HF spontaneously isomerize into new species. Interestingly, the protonation of **1** by HF carried out with diluted hydrofluoric acid resulted in the formation of the tetranuclear complex **8**. This has been explained admitting that, under the described experimental conditions, a significant amount of the species  $\{\text{F}(\text{HF})\}^-$ , or  $\{\text{F}(\text{H}_2\text{O})_n\}^-$ , able to deprotonate one of the PHCY<sub>2</sub> ligands, may be present in the reaction medium.

## EXPERIMENTAL SECTION

Complex **1** was prepared as described in ref 2. Other reagents were from commercial suppliers and were used without further purification. Although the starting complex **1** as well as all of the hydrido-bridged products were found to be air stable, all manipulations were carried out under a pure dinitrogen atmosphere, using freshly distilled and oxygen-free solvents. C, H, N elemental analyses were carried out on a VARIO MICRO-CHNSO elemental analyzer. Infrared spectra were recorded on a Bruker Vector 22 spectrometer.

NMR spectra were recorded on BRUKER Avance 400 spectrometer; frequencies are referenced to Me<sub>4</sub>Si (<sup>1</sup>H and <sup>13</sup>C), 85% H<sub>3</sub>PO<sub>4</sub> (<sup>31</sup>P),

H<sub>2</sub>PtCl<sub>6</sub> (<sup>195</sup>Pt), CFCl<sub>3</sub> (<sup>19</sup>F), and BF<sub>3</sub>·Et<sub>2</sub>O (<sup>11</sup>B). The signal attributions and coupling constant assessment were made on the basis of a multinuclear NMR analysis of each compound including, besides 1D spectra, <sup>1</sup>H–<sup>31</sup>P HMQC, <sup>1</sup>H–<sup>195</sup>Pt HMQC, <sup>31</sup>P{<sup>1</sup>H} COSY, and <sup>31</sup>P{<sup>1</sup>H} long-range COSY. The coupling constants not directly extractable from the monodimensional spectra were obtained and attributed by the tilts of the multiplets due to the “passive” nuclei<sup>32</sup> in the aforementioned 2D spectra. High resolution mass spectrometry (HR-MS) analyses were performed using a time-of-flight mass spectrometer equipped with an electrospray ion source (Bruker micrOTOF). All analyses were carried out in positive ion mode. The sample solutions were introduced by continuous infusion with the aid of a syringe pump at a flow rate of 180 μL/min. The instrument was operated at end plate offset –500 V and capillary –4500 V. Nebulizer pressure was 1.5 bar (N<sub>2</sub>), and the drying gas (N<sub>2</sub>) flow was 10 L/min. Capillary exit and skimmer 1 were 120 and 40 V, respectively. The drying gas temperature was set at 220 °C. The software used for the simulations is Bruker Daltonics DataAnalysis (version 3.3). The ESI-MS and MS/MS analyses were carried out on a triple quadrupole PE Sciex instrument (mod. API 365), equipped with a TurboSpray source.

For the complexes  $[\mathbf{2}\text{-L}]^{2+}$  (L = H<sub>2</sub>O, CH<sub>3</sub>CN, PhCN), the HR-MS(+) spectrogram showed a very intense peak at  $m/z = 1197.53$  corresponding to  $[\text{M} - \text{L} - \text{H}]^+$ , accompanied, when the analysis was carried out in chloroform, by a peak at 1233.51 Da corresponding to  $[\text{M} - \text{L} + \text{Cl}]^+$ . Both peaks gave isotopic patterns superimposable on those calculated on the basis of the proposed formulas. In the case of  $[\mathbf{2}\text{-H}_2\text{O}]^{2+}$  a weak peak at  $m/z 1214.53$  was present, attributable to the  $[\text{M} - \text{H}]^+$  ion. For  $[\mathbf{2}\text{-PPh}_3]^{2+}$ , the spectrogram showed an intense peak at  $m/z 1459.21$ , corresponding to the monocharged ion  $[\mathbf{2}\text{-PPh}_3]^+$  together with a weak peak at  $m/z 730.32$  corresponding to the doubly charged ion  $[\mathbf{2}\text{-PPh}_3]^{2+}$ , as indicated by the isotope pattern (see the Supporting Information).

**Computational Details.** DFT calculations have been performed using the Amsterdam density-functional (ADF) package.<sup>33</sup> The 1s orbital for C, O, and F; 1s–2p orbitals for P; and 1s–4f orbitals for Pt are kept frozen. For all main group atoms, the valence orbitals were expanded in an uncontracted triple-ζ Slater-type orbital (STO) basis set augmented with a polarization function. For platinum orbitals, we used a double-ζ STO basis set for 5s and 5p and a triple-ζ STO basis set for 5d and 6s. As polarization functions, we used one 6p function for Pt; one 4d for P; one 3d for C, O, and F; and one 2p for H.

The LDA exchange correlation potential and energy were used, together with the Vosko–Wilk–Nusair parametrization<sup>34</sup> for homogeneous electron gas correlation, including Becke’s nonlocal correction<sup>35</sup> to the local exchange expression and Perdew’s nonlocal correction<sup>36</sup> to the local expression of correlation energy. Since the relativistic effect is important in these Pt-containing dimers, the zero-order regular approximation formalism (ZORA) without the spin–orbit coupling has been included.<sup>37</sup> Previous calculations indicate that gradient-corrected functionals together with the ZORA approximation can predict reliable properties of metal dimers in comparison with the Dirac four-component-MP2 calculations.<sup>38</sup> Molecular structures of all considered complexes were optimized at this gradient-corrected relativistic level with the above basis set. Single point calculations were subsequently performed on the optimized geometries with a larger basis set obtained from the above one through the addition of a second polarization function, a 5f for Pt; a 4f for P, C, O and F; and one 3d for H. Solvent effects were taken into account employing the COSMO continuum solvent model,<sup>39</sup> in the standard parametrization implemented in the ADF program.<sup>40</sup> Free energies of solvation in *n*-hexane ( $\epsilon = 1.88$ ,  $R_{\text{probe}} = 3.74$ ), acetone ( $\epsilon = 20.7$ ,  $R_{\text{probe}} = 3.08$ ), and dichloromethane ( $\epsilon = 8.9$ ,  $R_{\text{probe}} = 2.94$ ) were calculated with the largest basis set on the optimized geometries of all considered molecules.

**Table 2. Crystallographic Data and Structural Refinement Details for [9][BF<sub>4</sub>]<sub>2</sub> and [2-CH<sub>3</sub>CN][BF<sub>4</sub>]<sub>2</sub>**

	[9][BF <sub>4</sub> ] <sub>2</sub>	[2-CH <sub>3</sub> CN][BF <sub>4</sub> ] <sub>2</sub>
empirical formula	C <sub>100</sub> H <sub>190</sub> B <sub>2</sub> Cl <sub>8</sub> F <sub>8</sub> O <sub>2</sub> P <sub>8</sub> Pt <sub>4</sub>	C <sub>50</sub> H <sub>95</sub> B <sub>2</sub> F <sub>8</sub> NOP <sub>4</sub> Pt <sub>2</sub>
formula mass	2909.86	1413.95
temp [K]	130(2)	110(2)
wavelength [Å]	0.71073	0.71073
cryst syst	monoclinic	monoclinic
space group	P2 <sub>1</sub> /c	P2 <sub>1</sub> /c
unit cell dimensions		
<i>a</i> [Å]	14.108(4)	12.9836(6)
<i>b</i> [Å]	26.736(7)	22.6964(11)
<i>c</i> [Å]	18.009(4)	19.8898(10)
$\beta$ [deg]	121.086(17)	91.215(2)
<i>V</i> [Å <sup>3</sup> ]	5817(3)	5859.8(5)
<i>Z</i>	2	4
<i>D</i> <sub>calcd.</sub> [Mg m <sup>-3</sup> ]	1.661	1.603
abs coeff [mm <sup>-1</sup> ]	5.145	4.939
$\theta$ range for data coll. [deg]	2.28–26.70	2.05–28.00
independent reflns ( <i>R</i> <sub>int</sub> )	12097 (0.0750)	14137 (0.1211)
observed reflns	36788	97869
data/params	12097/603	14137/618
goodness-of-fit on <i>F</i> <sup>2</sup>	1.008	1.019
<i>R</i> <sup>a</sup> ( <i>I</i> > 2 $\sigma$ ( <i>I</i> ))	0.0452	0.0529
<i>wR</i> <sub>2</sub> <sup>b</sup> (all data)	0.0998	0.0890
largest diff. peak/hole [e Å <sup>-3</sup> ]	1.498–1.600	1.605–2.156

<sup>a</sup>  $R = \sum ||F_o| - |F_c|| / \sum |F_o|$ . <sup>b</sup>  $wR_2 = [\sum w(F_o^2 - F_c^2)^2 / \sum w(F_o^2)^2]^{1/2}$ .

**X-Ray Crystallography**<sup>41</sup>. Crystal data, parameters for intensity data collection, and convergence results for [2-CH<sub>3</sub>CN][BF<sub>4</sub>]<sub>2</sub> and [9][BF<sub>4</sub>]<sub>2</sub> are compiled in Table 2. Diffraction quality crystals were obtained from a chilled acetonitrile solution ([2-CH<sub>3</sub>CN][BF<sub>4</sub>]<sub>2</sub>) or by slow evaporation of the solvent from a CH<sub>2</sub>Cl<sub>2</sub> solution ([9][BF<sub>4</sub>]<sub>2</sub>). Data were collected with Mo K $\alpha$  radiation (graphite monochromator,  $\lambda = 0.71073$  Å) on a Bruker D8 goniometer with a SMART CCD area detector on crystals of approximate dimensions 0.17 × 0.13 × 0.04 mm ([9][BF<sub>4</sub>]<sub>2</sub>) and 0.16 × 0.03 × 0.03 mm ([2-CH<sub>3</sub>CN][BF<sub>4</sub>]<sub>2</sub>). Multi-scan based absorption corrections were performed with the help of the program SADABS.<sup>42</sup> The structures were solved by direct methods and refined with full-matrix least squares on *F*<sup>2</sup>.<sup>43</sup>

[(PHCy<sub>2</sub>)(H<sub>2</sub>O)Pt( $\mu$ -PCy<sub>2</sub>)( $\mu$ -H)Pt(PHCy<sub>2</sub>){P(OH)Cy<sub>2</sub>}]<sub>2</sub>[BF<sub>4</sub>]<sub>2</sub>-(Pt-Pt) ([2-H<sub>2</sub>O][BF<sub>4</sub>]<sub>2</sub>). A total of 45  $\mu$ L of HBF<sub>4</sub>(aq) (50%<sub>w/w</sub>, 0.35 mmol) was added to an *n*-hexane solution of **1** (0.140 g, 0.12 mmol in 10 mL), and the resulting mixture was stirred for 2 h at room temperature, causing the precipitation of a pale yellow powder. Then, the solid was filtered off, washed with *n*-hexane (3 × 5 mL), and dried under vacuum conditions for 12 h. Yield: 0.14 g (95%).

The complex is very soluble in halogenated solvents and acetonitrile and insoluble in Et<sub>2</sub>O, *n*-hexane, and aromatic solvents.

Anal. Calcd for C<sub>48</sub>H<sub>93</sub>B<sub>2</sub>F<sub>8</sub>O<sub>2</sub>P<sub>4</sub>Pt<sub>2</sub>: C, 41.48; H, 6.74. Found: C, 41.35; H, 6.81. ESI-MS, exact mass for the dication C<sub>48</sub>H<sub>93</sub>O<sub>2</sub>P<sub>4</sub>Pt<sub>2</sub>: 1215.5421. Measured: *m/z* 1197.5333 (M - H<sub>2</sub>O - H)<sup>+</sup>; 1214.5272 (M - H)<sup>+</sup>.

IR (KBr, cm<sup>-1</sup>): 3364 (br, m),  $\nu$ (O-H + P-O-H); 2929 (vs), 2852 (vs), 2335 (br w),  $\nu$ (P-H); 2261 (w); 1635 (w)  $\nu$ ( $\mu$ -H-Pt); 1448 (s); 1344 (w); 1327 (w), 1295 (w); 1269 (m); 1074 (br vs),  $\nu$ (BF<sub>4</sub> + PO); 917 (s); 884 (s); 848 (s); 817 (m); 764 (w); 737 (m); 521 (s); 475 (m).

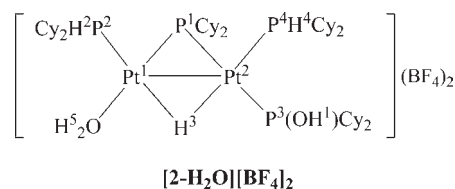
<sup>1</sup>H NMR (CD<sub>2</sub>Cl<sub>2</sub>, 258 K,  $\delta$ ): 6.33 (broad, H<sup>1</sup>), 5.34 (broad, H<sup>5</sup>), 4.58 (m, H<sup>2</sup>, <sup>1</sup>J<sub>H(2),P(2)}</sub> = 371 Hz, <sup>2</sup>J<sub>H(2),Pt(1)}</sub> = 193 Hz), 4.96 (m, H<sup>4</sup>, <sup>1</sup>J<sub>H(4),P(4)}</sub> = 362 Hz, <sup>2</sup>J<sub>H(4),Pt(2)}</sub> = 43 Hz), -5.48 (m, H<sup>3</sup>, <sup>2</sup>J<sub>H(3),P(4)}</sub> = 71 Hz, <sup>2</sup>J<sub>H(3),P(2)}</sub> = 63 Hz, <sup>2</sup>J<sub>H(3),P(1)}</sub> = 18 Hz, <sup>2</sup>J<sub>H(3),P(3)}</sub> = 16 Hz, <sup>1</sup>J<sub>H(3),Pt(2)}</sub> = 541 Hz, <sup>1</sup>J<sub>H(3),Pt(1)}</sub> = 397 Hz) ppm.

<sup>31</sup>P{<sup>1</sup>H} NMR (CD<sub>2</sub>Cl<sub>2</sub>, 295 K,  $\delta$ ): 149.7 (dd, P<sup>1</sup>, <sup>1</sup>J<sub>P(1),Pt(1)}</sub> = 2940 Hz, <sup>1</sup>J<sub>P(1),Pt(2)}</sub> = 1498 Hz, <sup>2</sup>J<sub>P(1),P(3)}</sub> = 289 Hz, <sup>2</sup>J<sub>P(1),P(4)}</sub> = 13 Hz), 126.8 (dd, P<sup>3</sup>, <sup>1</sup>J<sub>P(3),Pt(2)}</sub> = 2770 Hz, <sup>2</sup>J<sub>P(3),P(1)}</sub> = 289 Hz, <sup>2</sup>J<sub>P(3),P(4)}</sub> = 23 Hz), 9.1 (d, P<sup>2</sup>, <sup>1</sup>J<sub>P(2),Pt(1)}</sub> = 4047 Hz, <sup>2</sup>J<sub>P(2),Pt(2)}</sub> = 206 Hz, <sup>3</sup>J<sub>P(2),P(4)}</sub> = 45 Hz), -1.7 (broad, P<sup>4</sup>, <sup>1</sup>J<sub>P(4),Pt(2)}</sub> = 3414 Hz, <sup>2</sup>J<sub>P(4),Pt(1)}</sub> = 206 Hz, <sup>2</sup>J<sub>P(4),Pt(1)}</sub> = 13 Hz, <sup>2</sup>J<sub>P(4),P(3)}</sub> = 23 Hz, <sup>3</sup>J<sub>P(4),P(2)}</sub> = 45 Hz) ppm.

<sup>195</sup>Pt{<sup>1</sup>H} NMR (CD<sub>2</sub>Cl<sub>2</sub>, 258 K,  $\delta$ ): -5589 (m, Pt<sup>1</sup>, <sup>1</sup>J<sub>Pt(1),P(2)}</sub> = 4047 Hz, <sup>1</sup>J<sub>Pt(1),P(1)}</sub> = 2940 Hz, <sup>2</sup>J<sub>Pt(1),P(4)}</sub> = 206 Hz, <sup>1</sup>J<sub>Pt(1),Pt(2)}</sub> = 714 Hz), -5302 (m, Pt<sup>2</sup>, <sup>1</sup>J<sub>Pt(2),P(4)}</sub> = 3414 Hz, <sup>1</sup>J<sub>Pt(2),P(3)}</sub> = 2770 Hz, <sup>1</sup>J<sub>Pt(2),P(1)}</sub> = 1498 Hz, <sup>2</sup>J<sub>Pt(2),P(2)}</sub> = 206 Hz, <sup>1</sup>J<sub>Pt(2),Pt(1)}</sub> = 714 Hz) ppm.

<sup>11</sup>B{<sup>1</sup>H} NMR (CDCl<sub>3</sub>, 298 K,  $\delta$ ): -0.95 ppm.

<sup>19</sup>F NMR (CD<sub>2</sub>Cl<sub>2</sub>, 298 K,  $\delta$ ): -158.3 ppm.



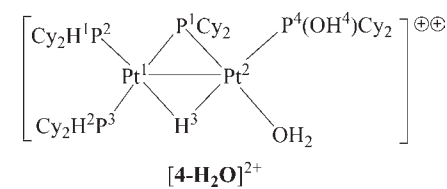
[(PHCy<sub>2</sub>)<sub>2</sub>Pt( $\mu$ -PCy<sub>2</sub>)( $\mu$ -H)Pt{P(OH)Cy<sub>2</sub>}(H<sub>2</sub>O)][BF<sub>4</sub>]<sub>2</sub>(Pt-Pt) ([4-H<sub>2</sub>O][BF<sub>4</sub>]<sub>2</sub>). An NMR tube charged with 60 mg of [2-H<sub>2</sub>O][BF<sub>4</sub>]<sub>2</sub> in 0.5 mL of CD<sub>2</sub>Cl<sub>2</sub> was sealed under nitrogen and allowed to stand at room temperature. Periodically recording <sup>31</sup>P-{<sup>1</sup>H} NMR spectra revealed the quantitative transformation into [4-H<sub>2</sub>O][BF<sub>4</sub>]<sub>2</sub> after 1 month. The recovered solution was concentrated to ca. 0.2 mL, and cold *n*-hexane was added, causing the precipitation of pure [4-H<sub>2</sub>O][BF<sub>4</sub>]<sub>2</sub> (50 mg, 83%).

IR (KBr, cm<sup>-1</sup>): 3222 (br, s)  $\nu$ (O-H); 2926 (s), 2926 (s); 2350 (w), 2343 (br w)  $\nu$ (P-H); 2261 (vw)  $\nu$ (P-O-H); 1634 (w)  $\nu$ ( $\mu$ -H-Pt); 1448 (s); 1346 (w); 1327 (w), 1295 (w); 1270 (m); 1058 (br vs),  $\nu$ (BF<sub>4</sub> + PO); 917 (s); 886 (m); 848 (s); 818 (m); 736 (m); 533 (m); 522 (s); 473 (m).

<sup>1</sup>H NMR (CD<sub>2</sub>Cl<sub>2</sub>, 295 K,  $\delta$ ): 5.9 (broad, POH + Pt-OH<sub>2</sub>), 4.99 (d, H<sup>1</sup>, <sup>1</sup>J<sub>H,P}</sub> = 368 Hz, <sup>2</sup>J<sub>H,Pt}</sub> = 63 Hz), 4.52 (m, H<sup>2</sup>, <sup>1</sup>J<sub>H,P}</sub> = 343 Hz, <sup>2</sup>J<sub>H,Pt}</sub> = 53 Hz), -6.29 (m, H<sup>3</sup>, <sup>2</sup>J<sub>H(3),P(2)}</sub> = 76 Hz, <sup>2</sup>J<sub>H(3),P(4)}</sub> = 65 Hz, <sup>2</sup>J<sub>H(3),P(1)}</sub> = 14 Hz, <sup>2</sup>J<sub>H(3),P(3)}</sub> = 14 Hz, <sup>1</sup>J<sub>H(3),Pt(1)}</sub> = 524 Hz, <sup>1</sup>J<sub>H(3),Pt(2)}</sub> = 386 Hz) ppm.

<sup>31</sup>P{<sup>1</sup>H} NMR (CD<sub>2</sub>Cl<sub>2</sub>, 295 K,  $\delta$ ): 141.6 (dt, P<sup>1</sup>, <sup>1</sup>J<sub>P(1),Pt(1)}</sub> = 1607 Hz, <sup>1</sup>J<sub>P(1),Pt(2)}</sub> = 3202 Hz, <sup>2</sup>J<sub>P(1),P(3)}</sub> = 229 Hz, <sup>2</sup>J<sub>P(1),P(2)}</sub>  $\approx$  <sup>2</sup>J<sub>P(1),P(4)}</sub> = 11 Hz), 118.5 (dd, P<sup>3</sup>, <sup>1</sup>J<sub>P(4),Pt(2)}</sub> = 3871 Hz, <sup>2</sup>J<sub>P(4),Pt(1)}</sub> = 212 Hz, <sup>3</sup>J<sub>P(4),P(2)}</sub> = 38 Hz, <sup>2</sup>J<sub>P(4),P(1)}</sub> = 11 Hz), 5.3 (dd, P<sup>2</sup>, <sup>1</sup>J<sub>P(3),Pt(1)}</sub> = 2125 Hz, <sup>2</sup>J<sub>P(3),Pt(2)}</sub> = 69 Hz, <sup>2</sup>J<sub>P(3),P(1)}</sub> = 229 Hz, <sup>2</sup>J<sub>P(3),P(2)}</sub> = 24 Hz), -6.1 (broad, P<sup>2</sup>, <sup>1</sup>J<sub>P(2),Pt(1)}</sub> = 3356 Hz, <sup>2</sup>J<sub>P(2),Pt(2)}</sub> = 118 Hz) ppm.

<sup>195</sup>Pt{<sup>1</sup>H} NMR (CD<sub>2</sub>Cl<sub>2</sub>, 295 K,  $\delta$ ): -5728 (dddd, Pt<sup>1</sup>, <sup>1</sup>J<sub>Pt(1),P(2)}</sub> = 3356 Hz, <sup>1</sup>J<sub>Pt(1),P(3)}</sub> = 2125 Hz, <sup>1</sup>J<sub>Pt(1),P(1)}</sub> = 1607 Hz, <sup>2</sup>J<sub>Pt(1),P(4)}</sub> = 212 Hz), -5291 (dddd, Pt<sup>2</sup>, <sup>1</sup>J<sub>Pt(2),P(4)}</sub> = 3871 Hz, <sup>1</sup>J<sub>Pt(2),P(1)}</sub> = 3202 Hz, <sup>2</sup>J<sub>Pt(2),P(2)}</sub> = 118 Hz, <sup>2</sup>J<sub>Pt(2),P(3)}</sub> = 69 Hz) ppm.



[(PHCy<sub>2</sub>)(CH<sub>3</sub>CN)Pt( $\mu$ -PCy<sub>2</sub>)( $\mu$ -H)Pt(PHCy<sub>2</sub>){P(OH)Cy<sub>2</sub>}]<sub>2</sub>[BF<sub>4</sub>]<sub>2</sub>(Pt-Pt) ([2-CH<sub>3</sub>CN][BF<sub>4</sub>]<sub>2</sub>). A total of 44  $\mu$ L of HBF<sub>4</sub>Me<sub>2</sub>O (0.43 mmol) was added to an *n*-hexane solution of **1** (0.20 g, 0.17 mmol



in 10 mL), causing the immediate precipitation of a yellow-orange solid. The resulting suspension was stirred for 20 min at room temperature. Then, the solid was filtered off, washed with Et<sub>2</sub>O (3 × 5 mL), and dried under vacuum conditions. The solid was dissolved in 5 mL of CH<sub>3</sub>CN, and the resulting yellow solution was stirred for 10 min. The solvent was then removed, and the compound [2-CH<sub>3</sub>CN][BF<sub>4</sub>]<sub>2</sub> was isolated as a pale yellow powder.

Yield: 0.18 g (75%).

The complex is hygroscopic; soluble in halogenated solvents and acetonitrile; and insoluble in Et<sub>2</sub>O, *n*-hexane, and aromatic solvents.

Anal. Calcd for C<sub>50</sub>H<sub>95</sub>B<sub>2</sub>F<sub>8</sub>NOP<sub>4</sub>Pt<sub>2</sub>: C, 42.47; H, 6.77; N, 0.99. Found: C, 42.65; H, 6.81; N, 1.03. ESI-MS, exact mass for the dication C<sub>50</sub>H<sub>95</sub>NOP<sub>4</sub>Pt<sub>2</sub>: 1239.5659. Measured: *m/z* 1197.5333 (M - CH<sub>3</sub>CN - H)<sup>+</sup>, 1233.5105 (M - CH<sub>3</sub>CN + Cl)<sup>+</sup>.

IR (KBr, cm<sup>-1</sup>): 3290 (broad w), ν(PO-H); 2931 (vs) 2852 (vs); 2324 (m), 2295 (m), ν(P-H + CN); 1651 (br m) ν(μ H-Pt); 1450 (s); 1411 (w); 1373 (w); 1346 (w); 1327 (w), 1296 (m); 1271 (m); 1203 (w); 1174 (m); 1073 (br vs), ν(BF<sub>4</sub> + PO); 918 (s); 884 (s); 849 (m); 818 (m); 762 (w); 737 (m); 521 (s); 474 (m).

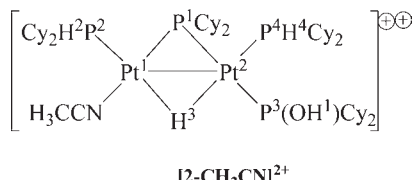
<sup>1</sup>H NMR (CD<sub>3</sub>CN, δ): 4.98 (m, H<sup>2</sup>, <sup>1</sup>J<sub>H(2),Pt(1)</sub> = 167 Hz), 5.22 (m, H<sup>4</sup>, <sup>1</sup>J<sub>H(4),Pt(4)</sub> = 379 Hz, <sup>2</sup>J<sub>H(4),Pt(2)</sub> = 44 Hz), -6.50 (m, H<sup>3</sup>, <sup>2</sup>J<sub>H(3),Pt(4)</sub> = 66 Hz, <sup>2</sup>J<sub>H(3),Pt(2)</sub> = 63 Hz, <sup>2</sup>J<sub>H(3),Pt(1)</sub> = 17 Hz, <sup>2</sup>J<sub>H(3),Pt(3)</sub> = 13 Hz, <sup>1</sup>J<sub>H(3),Pt(2)</sub> = 514 Hz, <sup>1</sup>J<sub>H(3),Pt(1)</sub> = 392 Hz), 6.6 (dd, <sup>44</sup>H<sup>1</sup>, <sup>2</sup>J<sub>H(1),Pt(3)</sub> = 12 Hz, <sup>2</sup>J<sub>H(1),Pt(1)</sub> = 6 Hz, <sup>3</sup>J<sub>H(1),Pt(2)</sub> = 64 Hz) ppm.

<sup>1</sup>H NMR (CDCl<sub>3</sub>, δ): 2.72 (CH<sub>3</sub>CN) ppm.

<sup>13</sup>C{<sup>1</sup>H} NMR (CDCl<sub>3</sub>, δ): 3.7 (CH<sub>3</sub>CN), 127 (CH<sub>3</sub>CN) ppm.

<sup>31</sup>P{<sup>1</sup>H} NMR (CD<sub>3</sub>CN, δ): 155.3 (dd, P<sup>1</sup>, <sup>1</sup>J<sub>P(1),Pt(1)</sub> = 2674 Hz, <sup>1</sup>J<sub>P(1),Pt(2)</sub> = 1485 Hz, <sup>2</sup>J<sub>P(1),Pt(3)</sub> = 290 Hz, <sup>2</sup>J<sub>P(1),Pt(4)</sub> = 13 Hz), 126.8 (dd, P<sup>3</sup>, <sup>1</sup>J<sub>P(3),Pt(2)</sub> = 2764 Hz, <sup>2</sup>J<sub>P(3),Pt(1)</sub> = 50 Hz, <sup>2</sup>J<sub>P(3),Pt(1)</sub> = 290 Hz, <sup>2</sup>J<sub>P(3),Pt(4)</sub> = 26 Hz), 0.6 (d, P<sup>2</sup>, <sup>1</sup>J<sub>P(2),Pt(1)</sub> = 3820 Hz, <sup>2</sup>J<sub>P(2),Pt(2)</sub> = 176 Hz, <sup>3</sup>J<sub>P(2),Pt(4)</sub> = 42 Hz), -2.2 (broad, P<sup>4</sup>, <sup>1</sup>J<sub>P(4),Pt(2)</sub> = 3437 Hz, <sup>2</sup>J<sub>P(4),Pt(1)</sub> = 176 Hz, <sup>2</sup>J<sub>P(4),Pt(1)</sub> = 13 Hz, <sup>2</sup>J<sub>P(4),Pt(3)</sub> = 26 Hz, <sup>3</sup>J<sub>P(4),Pt(2)</sub> = 42 Hz) ppm.

<sup>195</sup>Pt{<sup>1</sup>H} NMR (CD<sub>3</sub>CN, δ): -5653 (dddd, Pt<sup>1</sup>, <sup>1</sup>J<sub>Pt(1),Pt(2)</sub> = 3820 Hz, <sup>1</sup>J<sub>Pt(1),Pt(1)</sub> = 2674 Hz, <sup>2</sup>J<sub>Pt(1),Pt(3)</sub> = 50 Hz, <sup>2</sup>J<sub>Pt(1),Pt(4)</sub> = 176 Hz, <sup>1</sup>J<sub>Pt(1),Pt(2)</sub> = 929 Hz), -5512 (dddd, Pt<sup>2</sup>, <sup>1</sup>J<sub>Pt(2),Pt(4)</sub> = 3437 Hz, <sup>1</sup>J<sub>Pt(2),Pt(3)</sub> = 2764 Hz, <sup>1</sup>J<sub>Pt(2),Pt(1)</sub> = 1485 Hz, <sup>2</sup>J<sub>Pt(2),Pt(2)</sub> = 176 Hz, <sup>1</sup>J<sub>Pt(2),Pt(1)</sub> = 929 Hz) ppm.



[(PHC<sub>2</sub>)(PhCN)Pt(μ-PC<sub>2</sub>)(μ-H)Pt(PHC<sub>2</sub>){P(OH)C<sub>2</sub>}]<sub>2</sub>[BF<sub>4</sub>]<sub>2</sub>(Pt-Pt) ([2-PhCN][BF<sub>4</sub>]<sub>2</sub>). A total of 8 μL of benzonitrile was added to a CH<sub>2</sub>Cl<sub>2</sub> solution of [2-H<sub>2</sub>O][BF<sub>4</sub>]<sub>2</sub> (0.080 g, 0.058 mmol in 1.0 mL), and the resulting solution was stirred for 30 min at room temperature. After concentration of the solution to ca. 0.5 mL and the addition of *n*-hexane (2.0 mL), the resulting yellow solid was separated, washed with *n*-hexane (3 × 1 mL), and dried under vacuum conditions.

Yield: 0.068 g (79%).

The complex is hygroscopic; soluble in halogenated solvents; and insoluble in Et<sub>2</sub>O, *n*-hexane, and aromatic solvents.

Anal. Calcd for C<sub>55</sub>H<sub>96</sub>B<sub>2</sub>F<sub>8</sub>NOP<sub>4</sub>Pt<sub>2</sub>: C, 44.79; H, 6.56; N, 0.95. Found: C, 44.65; H, 6.81; N, 1.03.

ESI-MS, exact mass for the dication C<sub>55</sub>H<sub>96</sub>NOP<sub>4</sub>Pt<sub>2</sub>: 1300.5738. Measured: *m/z* 1197.5445 (M - PhCN - H)<sup>+</sup> and 1311.5338 (M - PhCN + Cl)<sup>+</sup>.

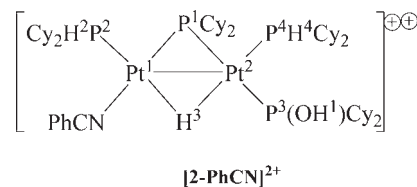
IR (KBr, cm<sup>-1</sup>): 3222 (br w), ν(PO-H); 2927 (vs) 2851 (vs); 2260 (m), ν(P-H+CN); 1630 (w) ν(μ H-Pt); 1594 (w); 1488 (w); 1449 (s) 1345 (w); 1327 (w), 1295 (w); 1271 (m); 1201 (m); 1180 (s); 1059

(br vs), ν(BF<sub>4</sub> + PO); 1003 (s), 916 (s); 884 (s); 848 (s); 817 (m); 760 (m); 735 (m); 684 (m), 520 (s); 473 (s).

<sup>1</sup>H NMR (CDCl<sub>3</sub>, 295 K, δ): 7.94–7.66 (m, arom), 5.10 (m, H<sup>2</sup>, <sup>1</sup>J<sub>H(2),Pt(2)</sub> = 388 Hz, <sup>2</sup>J<sub>H(2),Pt(1)</sub> = 166 Hz), 4.99 (m, H<sup>4</sup>, <sup>1</sup>J<sub>H(4),Pt(4)</sub> = 373 Hz, <sup>2</sup>J<sub>H(4),Pt(2)</sub> = 41 Hz), -6.370 (m, H<sup>3</sup>, <sup>2</sup>J<sub>H(3),Pt(4)</sub> = 64 Hz, <sup>2</sup>J<sub>H(3),Pt(2)</sub> = 62 Hz, <sup>2</sup>J<sub>H(3),Pt(1)</sub> = 17 Hz, <sup>2</sup>J<sub>H(3),Pt(3)</sub> = 11 Hz, <sup>1</sup>J<sub>H(3),Pt(2)</sub> = 510 Hz, <sup>1</sup>J<sub>H(3),Pt(1)</sub> = 402 Hz), 7.5 (broad, H<sup>1</sup>) ppm.

<sup>31</sup>P{<sup>1</sup>H} NMR (CDCl<sub>3</sub>, 295 K, δ): 155.8 (m, P<sup>1</sup>, <sup>1</sup>J<sub>P(1),Pt(1)</sub> = 2656 Hz, <sup>1</sup>J<sub>P(1),Pt(2)</sub> = 1477 Hz, <sup>2</sup>J<sub>P(1),Pt(3)</sub> = 289 Hz, <sup>2</sup>J<sub>P(1),Pt(4)</sub> = 12 Hz), 126.0 (d, P<sup>3</sup>, <sup>1</sup>J<sub>P(3),Pt(2)</sub> = 2772 Hz, <sup>2</sup>J<sub>P(3),Pt(1)</sub> = 289 Hz), 1.4 (d, P<sup>2</sup>, <sup>1</sup>J<sub>P(2),Pt(1)</sub> = 3799 Hz, <sup>2</sup>J<sub>P(2),Pt(2)</sub> = 171 Hz, <sup>3</sup>J<sub>P(2),Pt(4)</sub> = 40 Hz), 0.5 (broad, P<sup>4</sup>, <sup>1</sup>J<sub>P(4),Pt(2)</sub> = 3508 Hz, <sup>2</sup>J<sub>P(4),Pt(1)</sub> = 172 Hz) ppm.

<sup>195</sup>Pt{<sup>1</sup>H} NMR (CDCl<sub>3</sub>, 295 K, δ): -5651 (ddd, Pt<sup>1</sup>, <sup>1</sup>J<sub>Pt(1),Pt(2)</sub> = 3799 Hz, <sup>1</sup>J<sub>Pt(1),Pt(1)</sub> = 2656 Hz, <sup>2</sup>J<sub>Pt(1),Pt(4)</sub> = 172 Hz, <sup>1</sup>J<sub>Pt(1),Pt(2)</sub> = 929 Hz), -5484 (dddd, Pt<sup>2</sup>, <sup>1</sup>J<sub>Pt(2),Pt(4)</sub> = 3508 Hz, <sup>1</sup>J<sub>Pt(2),Pt(3)</sub> = 2772 Hz, <sup>1</sup>J<sub>Pt(2),Pt(1)</sub> = 1477 Hz, <sup>2</sup>J<sub>Pt(2),Pt(2)</sub> = 171 Hz, <sup>1</sup>J<sub>Pt(2),Pt(1)</sub> = 929 Hz) ppm.



[(PHC<sub>2</sub>)(PPh<sub>3</sub>)Pt(μ-PC<sub>2</sub>)(μ-H)Pt(PHC<sub>2</sub>){P(OH)C<sub>2</sub>}]<sub>2</sub>[BF<sub>4</sub>]<sub>2</sub>(Pt-Pt) ([2-PPh<sub>3</sub>][BF<sub>4</sub>]<sub>2</sub>). A total of 15 mg of PPh<sub>3</sub> (0.057 mmol) was added to a CH<sub>2</sub>Cl<sub>2</sub> solution of [2-H<sub>2</sub>O][BF<sub>4</sub>]<sub>2</sub> (0.069 g, 0.050 mmol in 1.0 mL), and the resulting mixture was stirred for 10 min at room temperature. After concentration of the solution to ca. 0.5 mL and the addition of *n*-hexane (2.0 mL), the resulting yellow solid was separated, washed with *n*-hexane (3 × 1 mL), and dried under vacuum conditions.

Yield: 0.053 g (70%).

The complex is hygroscopic; soluble in halogenated solvents; and insoluble in Et<sub>2</sub>O, *n*-hexane, and aromatic solvents.

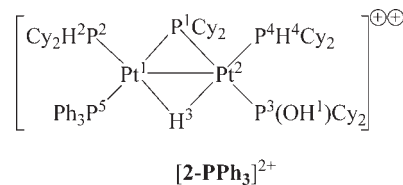
Anal. Calcd for C<sub>66</sub>H<sub>106</sub>B<sub>2</sub>F<sub>8</sub>OP<sub>5</sub>Pt<sub>2</sub>: C, 48.51; H, 6.54. Found: C, 48.27; H, 6.24. ESI-MS, exact mass for the dication C<sub>66</sub>H<sub>106</sub>OP<sub>5</sub>Pt<sub>2</sub>: 1459.6227. Measured: *m/z* 1459.2128 (M)<sup>+</sup>.

IR (KBr, cm<sup>-1</sup>): 3215 (br m), ν(PO-H); 2929 (vs), 2852 (s); 2350 (w) 2261 (w); 1634 (w) ν(μ H-Pt); 1588 (w); 1483 (m); 1442 (s); 1294 (w); 1270 (m); 1203 (w); 1180 (s); 1096 (br vs), ν(BF<sub>4</sub> + PO); 1001 (s); 918 (s); 884 (s); 848 (m); 816 (s); 747 (s); 697 (s); 512 (s); 490 (m).

<sup>1</sup>H NMR (CDCl<sub>3</sub>, 295 K, δ): 7.81–7.35 (m, arom), 5.04 (m, H<sup>2</sup>, <sup>1</sup>J<sub>H(2),Pt(2)</sub> = 365 Hz), 5.13 (m, H<sup>4</sup>, <sup>1</sup>J<sub>H(4),Pt(4)</sub> = 367 Hz, <sup>2</sup>J<sub>H(4),Pt(2)</sub> = 57 Hz), -5.97 (m, H<sup>3</sup>, <sup>2</sup>J<sub>H(3),Pt(2)</sub> ≈ <sup>2</sup>J<sub>H(3),Pt(4)</sub> = 62 Hz, <sup>2</sup>J<sub>H(3),Pt(1)</sub> ≈ <sup>2</sup>J<sub>H(3),Pt(3)</sub> ≈ <sup>2</sup>J<sub>H(3),Pt(5)</sub> = 13 Hz, <sup>1</sup>J<sub>H(3),Pt(1)</sub> = 470 Hz, <sup>1</sup>J<sub>H(3),Pt(2)</sub> = 484 Hz), 6.1 (broad, H<sup>1</sup>) ppm.

<sup>31</sup>P{<sup>1</sup>H} NMR (CDCl<sub>3</sub>, 295 K, δ): 171.9 (dd, P<sup>1</sup>, <sup>1</sup>J<sub>P(1),Pt(2)</sub> = 1635 Hz, <sup>1</sup>J<sub>P(1),Pt(1)</sub> = 1442 Hz, <sup>2</sup>J<sub>P(1),Pt(5)</sub> = 225 Hz, <sup>2</sup>J<sub>P(1),Pt(3)</sub> = 270 Hz), 123.7 (d, P<sup>3</sup>, <sup>1</sup>J<sub>P(3),Pt(2)</sub> = 2898 Hz, <sup>2</sup>J<sub>P(3),Pt(1)</sub> = 270 Hz), 4.5 (d, P<sup>5</sup>, <sup>1</sup>J<sub>P(5),Pt(1)</sub> = 2420 Hz, <sup>2</sup>J<sub>P(5),Pt(1)</sub> = 225 Hz), -1.7 (broad, P<sup>2</sup>, <sup>1</sup>J<sub>P(2),Pt(1)</sub> = 3555 Hz, <sup>2</sup>J<sub>P(2),Pt(2)</sub> = 170 Hz), -3.1 (broad, P<sup>4</sup>, <sup>1</sup>J<sub>P(5),Pt(2)</sub> = 3494 Hz) ppm.

<sup>195</sup>Pt{<sup>1</sup>H} NMR (CDCl<sub>3</sub>, 295 K, δ): -5705 (m, Pt<sup>1</sup>, <sup>1</sup>J<sub>Pt(1),Pt(1)</sub> = 1635 Hz, <sup>1</sup>J<sub>Pt(1),Pt(2)</sub> = 3555 Hz, <sup>1</sup>J<sub>Pt(1),Pt(5)</sub> = 2420 Hz), -5684 (m, Pt<sup>2</sup>, <sup>1</sup>J<sub>Pt(2),Pt(1)</sub> = 1442 Hz, <sup>1</sup>J<sub>Pt(2),Pt(3)</sub> = 2898 Hz, <sup>1</sup>J<sub>Pt(2),Pt(4)</sub> = 3494 Hz) ppm.

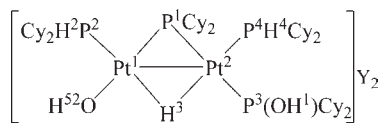


**Reactions of 1 with HF.** In a PTFE NMR tube, a CD<sub>2</sub>Cl<sub>2</sub> solution of **1** (0.040 g, 0.033 mmol in 0.5 mL) was added to 60 μL of HF (50%<sub>w</sub>, *d* = 1.155 g/mL) and vigorously shaken for 5 min. Multinuclear NMR analysis revealed the quantitative transformation into [2-H<sub>2</sub>O](Y)<sub>2</sub> (spectroscopic yield > 90%). On standing in solution, part of [2-H<sub>2</sub>O](Y)<sub>2</sub> transformed into [6](Y) (1 h), which, in turn, evolved, in the presence of excess HF, into [7](Y) (ca. 24 h).

**NMR Features of [(PHCY<sub>2</sub>)(H<sub>2</sub>O)Pt(μ-PCy<sub>2</sub>)(μ-H)Pt(PHCY<sub>2</sub>){P(OH)Cy<sub>2</sub>}]<sub>2</sub>(Y)<sub>2</sub>(Pt-Pt) ([2-H<sub>2</sub>O](Y)<sub>2</sub>).** <sup>1</sup>H NMR (CD<sub>2</sub>Cl<sub>2</sub>, 298 K, δ): 4.65 (m, H<sup>2</sup>, <sup>1</sup>J<sub>H(2),P(2)</sub> = 365 Hz, <sup>2</sup>J<sub>H(2),Pt(1)</sub> = 200 Hz), 5.05 (m, H<sup>4</sup>, <sup>1</sup>J<sub>H(4),P(4)</sub> = 366 Hz, <sup>2</sup>J<sub>H(4),Pt(2)</sub> = 41 Hz), -5.37 (m, H<sup>3</sup>, <sup>2</sup>J<sub>H(3),P(4)</sub> = 68 Hz, <sup>2</sup>J<sub>H(3),P(2)</sub> = 73 Hz, <sup>2</sup>J<sub>H(3),P(1)</sub> = 15 Hz, <sup>2</sup>J<sub>H(3),P(3)</sub> = 16 Hz, <sup>1</sup>J<sub>H(3),Pt(2)</sub> = 566 Hz, <sup>1</sup>J<sub>H(3),Pt(1)</sub> = 402 Hz) ppm.

<sup>31</sup>P{<sup>1</sup>H} NMR (CD<sub>2</sub>Cl<sub>2</sub>, 298 K, δ): 140.8 (broad d, P<sup>1</sup>, <sup>1</sup>J<sub>P(1),Pt(1)</sub> = 2886 Hz, <sup>1</sup>J<sub>P(1),Pt(2)</sub> = 1461 Hz, <sup>2</sup>J<sub>P(1),P(3)</sub> = 294 Hz), 117.8 (d, P<sup>3</sup>, <sup>1</sup>J<sub>P(3),Pt(2)</sub> = 2712 Hz, <sup>2</sup>J<sub>P(3),P(1)</sub> = 294 Hz), 12.8 (d, P<sup>2</sup>, <sup>1</sup>J<sub>P(2),Pt(1)</sub> = 4158 Hz, <sup>2</sup>J<sub>P(2),Pt(2)</sub> = 211 Hz, <sup>3</sup>J<sub>P(2),P(4)</sub> = 45 Hz), 3.4 (broad, P<sup>4</sup>, <sup>1</sup>J<sub>P(4),Pt(2)</sub> = 3496 Hz, <sup>2</sup>J<sub>P(4),Pt(1)</sub> = 165 Hz) ppm.

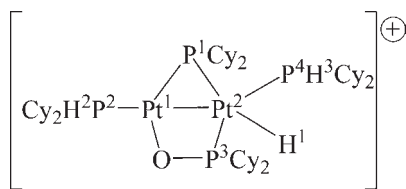
<sup>195</sup>Pt{<sup>1</sup>H} NMR (CD<sub>2</sub>Cl<sub>2</sub>, 298 K, δ): -5540 (m, Pt<sup>1</sup>, <sup>1</sup>J<sub>Pt(1),P(2)</sub> = 4043 Hz, <sup>1</sup>J<sub>Pt(1),P(1)</sub> = 2886 Hz, <sup>2</sup>J<sub>Pt(1),P(4)</sub> = 165 Hz), -5147 (m, Pt<sup>2</sup>, <sup>1</sup>J<sub>Pt(2),P(4)</sub> = 3496 Hz, <sup>1</sup>J<sub>Pt(2),P(3)</sub> = 2712 Hz, <sup>1</sup>J<sub>Pt(2),P(1)</sub> = 1461 Hz, <sup>2</sup>J<sub>Pt(2),P(2)</sub> = 221 Hz) ppm.

[2-H<sub>2</sub>O]Y<sub>2</sub>

**NMR Features of [6](Y).** <sup>1</sup>H NMR (CD<sub>2</sub>Cl<sub>2</sub>, 298 K, δ): 4.90 (m, H<sup>2</sup>, <sup>1</sup>J<sub>H(2),P(2)</sub> = 369 Hz, <sup>1</sup>J<sub>H(2),Pt(1)</sub> = 140 Hz), 5.40 (m, H<sup>3</sup>, <sup>1</sup>J<sub>H(3),P(4)</sub> = 360 Hz), -1.61 (dddd, H<sup>1</sup>, <sup>2</sup>J<sub>H(1),P(1)</sub> = 105 Hz, <sup>2</sup>J<sub>H(1),P(4)</sub> = 19 Hz, <sup>2</sup>J<sub>H(1),P(4)</sub> = 16 Hz, <sup>2</sup>J<sub>H(1),P(2)</sub> = 8 Hz, <sup>1</sup>J<sub>H(1),Pt(2)</sub> = 832 Hz, <sup>2</sup>J<sub>H(1),Pt(1)</sub> = 50 Hz) ppm.

<sup>31</sup>P{<sup>1</sup>H} NMR (CD<sub>2</sub>Cl<sub>2</sub>, 298 K, δ): 182.0 (dd, P<sup>1</sup>, <sup>1</sup>J<sub>P(1),Pt(1)</sub> = 3529 Hz, <sup>1</sup>J<sub>P(1),Pt(2)</sub> = 1483 Hz, <sup>2</sup>J<sub>P(1),P(2)</sub> = 44 Hz, <sup>2</sup>J<sub>P(1),P(4)</sub> = 16 Hz), 80.6 (dd, P<sup>3</sup>, <sup>1</sup>J<sub>P(3),Pt(2)</sub> = 1425 Hz, <sup>2</sup>J<sub>P(3),Pt(1)</sub> = 250 Hz, <sup>2</sup>J<sub>P(3),P(4)</sub> = 157 Hz, <sup>3</sup>J<sub>P(3),P(2)</sub> = 56 Hz), 9.4 (m, P<sup>2</sup>, <sup>1</sup>J<sub>P(2),Pt(1)</sub> = 4868 Hz, <sup>2</sup>J<sub>P(2),Pt(2)</sub> = 40 Hz, <sup>2</sup>J<sub>P(2),P(1)</sub> = 44 Hz, <sup>2</sup>J<sub>P(2),P(3)</sub> = 56 Hz, <sup>3</sup>J<sub>P(2),P(4)</sub> = 40 Hz), -5.7 (m, P<sup>4</sup>, <sup>1</sup>J<sub>P(4),Pt(2)</sub> = 2451 Hz, <sup>2</sup>J<sub>P(4),P(1)</sub> = 16 Hz, <sup>3</sup>J<sub>P(4),P(2)</sub> = 40 Hz, <sup>2</sup>J<sub>P(4),P(3)</sub> = 157 Hz).

<sup>195</sup>Pt{<sup>1</sup>H} NMR (CD<sub>2</sub>Cl<sub>2</sub>, 298 K, δ): -5147 (ddd, Pt<sup>1</sup>, <sup>1</sup>J<sub>Pt(1),P(1)</sub> = 3529 Hz, <sup>1</sup>J<sub>Pt(1),P(2)</sub> = 4868 Hz, <sup>2</sup>J<sub>Pt(1),P(3)</sub> = 250 Hz), -5983 (dddd, Pt<sup>2</sup>, <sup>1</sup>J<sub>Pt(2),P(1)</sub> = 1483 Hz, <sup>1</sup>J<sub>Pt(2),P(3)</sub> = 1425 Hz, <sup>1</sup>J<sub>Pt(2),P(4)</sub> = 2451 Hz, <sup>2</sup>J<sub>Pt(2),P(2)</sub> = 40 Hz) ppm.

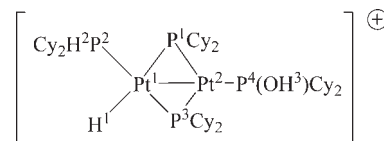
[6]<sup>+</sup>

**NMR Features of [7](Y).** <sup>1</sup>H NMR (CD<sub>2</sub>Cl<sub>2</sub>, 298 K, δ): 6.1 (broad, H<sup>3</sup>) 5.57 (m, H<sup>2</sup>, <sup>1</sup>J<sub>H(2),P(2)</sub> = 352 Hz, <sup>1</sup>J<sub>H(2),Pt(1)</sub> = 23 Hz), -2.84 (m, H<sup>1</sup>, <sup>2</sup>J<sub>H(1),P(1)</sub> = 106 Hz, <sup>3</sup>J<sub>H(1),P(4)</sub> = 29 Hz, <sup>2</sup>J<sub>H(1),P(2)</sub> = 23 Hz, <sup>2</sup>J<sub>H(1),P(3)</sub> = 10 Hz, <sup>1</sup>J<sub>H(1),Pt(1)</sub> = 833 Hz) ppm.

<sup>31</sup>P{<sup>1</sup>H} NMR (CD<sub>2</sub>Cl<sub>2</sub>, 298 K, δ): 299.6 (ddd, P<sup>1</sup>, <sup>1</sup>J<sub>P(1),Pt(1)</sub> = 1150 Hz, <sup>1</sup>J<sub>P(1),Pt(2)</sub> = 2378 Hz, <sup>2</sup>J<sub>P(1),P(2)</sub> = 12 Hz, <sup>2</sup>J<sub>P(1),P(3)</sub> = 198 Hz, <sup>2</sup>J<sub>P(1),P(4)</sub> = 57 Hz), 294.3 (ddd, P<sup>3</sup>, <sup>1</sup>J<sub>P(3),Pt(1)</sub> = 1138 Hz, <sup>1</sup>J<sub>P(3),Pt(2)</sub> = 2552 Hz, <sup>2</sup>J<sub>P(3),P(2)</sub> = 170 Hz, <sup>2</sup>J<sub>P(3),P(1)</sub> = 198 Hz, <sup>2</sup>J<sub>P(3),P(4)</sub> = 69 Hz), 134.8

(ddd, P<sup>4</sup>, <sup>1</sup>J<sub>P(4),Pt(2)</sub> = 5396 Hz, <sup>2</sup>J<sub>P(4),P(1)</sub> = 57 Hz, <sup>2</sup>J<sub>P(4),P(2)</sub> = 36 Hz, <sup>3</sup>J<sub>P(4),P(3)</sub> = 69 Hz), 1.7 (dd, P<sup>2</sup>, <sup>1</sup>J<sub>P(2),Pt(1)</sub> = 2920 Hz, <sup>2</sup>J<sub>P(2),P(1)</sub> = 12 Hz, <sup>2</sup>J<sub>P(2),P(3)</sub> = 170 Hz, <sup>3</sup>J<sub>P(2),P(4)</sub> = 36 Hz) ppm.

<sup>195</sup>Pt{<sup>1</sup>H} NMR (CD<sub>2</sub>Cl<sub>2</sub>, 298 K, δ): -6152 (ddd, Pt<sup>1</sup>, <sup>1</sup>J<sub>Pt(1),P(1)</sub> = 1150 Hz, <sup>1</sup>J<sub>Pt(1),P(2)</sub> = 2920 Hz, <sup>1</sup>J<sub>Pt(1),P(3)</sub> = 1138 Hz), -5354 (ddd, Pt<sup>2</sup>, <sup>1</sup>J<sub>Pt(2),P(1)</sub> = 2378 Hz, <sup>1</sup>J<sub>Pt(2),P(3)</sub> = 2552 Hz, <sup>1</sup>J<sub>Pt(2),P(4)</sub> = 5396 Hz) ppm.

[7]<sup>+</sup>

**Reactions of [2-H<sub>2</sub>O][BF<sub>4</sub>]<sub>2</sub> with NaF.** A mixture of NaF (5 mg, 0.12 mmol) and [2-H<sub>2</sub>O][BF<sub>4</sub>]<sub>2</sub> (0.035 g, 0.025 mmol) in 2.0 mL water was sonicated at 298 K for 1 h. Extraction with 0.5 mL of CD<sub>2</sub>Cl<sub>2</sub> gave a yellow-orange solution which showed at the multinuclear NMR analysis the presence of [6]<sup>+</sup> as the main species.

**Formation of Tetranuclear Compounds.** *Synthesis of [(PHCY<sub>2</sub>){κP-P(O)Cy<sub>2</sub>}Pt<sup>1</sup>(μ-PCy<sub>2</sub>)(μ-H)Pt<sup>2</sup>(μ-PCy<sub>2</sub>)<sub>2</sub>(Pt<sup>1</sup>-Pt<sup>2</sup>)]<sub>2</sub>(Y)<sub>2</sub> (**8**). A PTFE NMR tube filled with a dichloromethane solution of **1** (80 mg, 0.067 mmol in 0.5 mL) was added to 40 μL of hydrofluoric acid (5%<sub>w</sub>), without stirring, and the resulting biphasic system was left at 298 K for 24 h. Then, the supernatant aqueous phase was sucked up by a cannula, and the organic phase was concentrated to ca. 0.2 mL. The addition of *n*-hexane caused the formation of a white solid (**8**), which was filtered off, washed with *n*-hexane, and dried under vacuum conditions. Yield: 32 mg (40%).*

Anal. Calcd for C<sub>96</sub>H<sub>180</sub>O<sub>2</sub>P<sub>8</sub>Pt<sub>4</sub>: C, 48.15; H, 7.58. Found: C, 47.95; H, 7.51. ESI-MS, exact mass for the cation [C<sub>96</sub>H<sub>181</sub>O<sub>2</sub>P<sub>8</sub>Pt<sub>4</sub>]<sup>+</sup>: 2395.04. Measured: *m/z* 2395.1 (M + H)<sup>+</sup>.

IR (KBr, cm<sup>-1</sup>): 2926 (vs), 2850 (vs), 2327 (br w) ν(P-H); 1636 (br w) ν(μ H-Pt); 1447 (s); 1343 (w); 1328 (w); 1292 (m); 1266 (m); 1192 (m) 1178 (s); 1104 (s); 1046 (m); 1002 (s) 919 (m); 886 (s); 849 (s); 817 (m); 734 (vs); 574 (m); 539 (m); 522 (m); 482 (s); 462 (s).

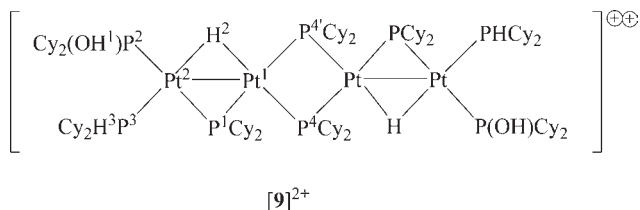
[(PHCY<sub>2</sub>){P(OH)Cy<sub>2</sub>}Pt<sup>1</sup>(μ-PCy<sub>2</sub>)(μ-H)Pt<sup>2</sup>(μ-PCy<sub>2</sub>)<sub>2</sub>][BF<sub>4</sub>]<sub>2</sub>(Pt<sup>1</sup>-Pt<sup>2</sup>) · 2CH<sub>2</sub>Cl<sub>2</sub> ([9][BF<sub>4</sub>]<sub>2</sub>). A CH<sub>2</sub>Cl<sub>2</sub> suspension of **8** (30 mg, 0.013 mmol in 1.0 mL) was added to 4 μL of HBF<sub>4</sub>Me<sub>2</sub>O and stirred for 5 min. The addition of *n*-hexane to the mixture caused the precipitation of a white solid ([9][BF<sub>4</sub>]<sub>2</sub>), which was filtered off, washed with *n*-hexane, and dried under vacuum conditions. Yield: 28 mg (87%).

IR (KBr, cm<sup>-1</sup>): 3180 (br w) ν(POH); 2928 (vs), 2852 (vs); 2264 (w); 1628 (w) ν(μ H-Pt); 1292 (m); 1266 (m); 1178 (m); 1101 (br vs) ν(BF<sub>4</sub> + PO); 1001 (s); 914 (s); 884 (s); 848 (m); 815 (m); 724 (s); 520 (s); 489 (s); 461 (s); 403 (m); 379 (s).

<sup>1</sup>H NMR (dmso-*d*<sub>6</sub>, 315 K, δ): 10.04 (s, H<sup>1</sup>, <sup>1</sup>J<sub>H(1),Pt(2)</sub> = 57 Hz), 5.73 (s, CH<sub>2</sub>Cl<sub>2</sub>), 5.28 (m, H<sup>3</sup>, <sup>1</sup>J<sub>H(3),P(3)</sub> = 355 Hz, <sup>2</sup>J<sub>H(3),Pt(2)</sub> = 65 Hz), -5.85 (m, H<sup>2</sup>, <sup>2</sup>J<sub>H(2),P(1)</sub> = 21 Hz, <sup>2</sup>J<sub>H(2),P(2)</sub> = 17 Hz, <sup>2</sup>J<sub>H(2),P(3)</sub> = 83 Hz, <sup>2</sup>J<sub>H(2),P(4)</sub> = 38 Hz, <sup>1</sup>J<sub>H(2),Pt(1)</sub> = 576 Hz, <sup>1</sup>J<sub>H(2),Pt(2)</sub> = 440 Hz) ppm.

<sup>31</sup>P{<sup>1</sup>H} NMR (CD<sub>2</sub>Cl<sub>2</sub>, 298 K, δ): 136.4 (m, P<sup>1</sup>, <sup>1</sup>J<sub>P(1),Pt(1)</sub> = 1700 Hz, <sup>1</sup>J<sub>P(1),Pt(2)</sub> = 1380 Hz, <sup>2</sup>J<sub>P(1),P(4)</sub> = 260 Hz, <sup>2</sup>J<sub>P(1),P(2)</sub> = 246 Hz, <sup>2</sup>J<sub>P(1),P(4)</sub> = 8 Hz, <sup>2</sup>J<sub>P(1),P(3)</sub> = 7 Hz), 121.5 (dd, P<sup>2</sup>, <sup>1</sup>J<sub>P(2),Pt(2)</sub> = 2828 Hz, <sup>2</sup>J<sub>P(2),Pt(1)</sub> = 40 Hz, <sup>2</sup>J<sub>P(2),P(1)</sub> = 246 Hz, <sup>2</sup>J<sub>P(2),P(3)</sub> = 15 Hz), 4.3 (broad, P<sup>3</sup>, <sup>1</sup>J<sub>P(3),Pt(2)</sub> = 3387 Hz, <sup>2</sup>J<sub>P(3),Pt(1)</sub> = 70 Hz, <sup>2</sup>J<sub>P(3),P(2)</sub> = 15 Hz, <sup>3</sup>J<sub>P(3),P(4)</sub> = 10 Hz, <sup>2</sup>J<sub>P(3),P(1)</sub> = 7 Hz), -110.5 (broad, P<sup>4</sup>, <sup>1</sup>J<sub>P(4),Pt(1)</sub> = 2550 Hz, <sup>2</sup>J<sub>P(4),Pt(2)</sub> = 91 Hz, <sup>1</sup>J<sub>P(4),Pt(1)</sub> = 1850 Hz, <sup>2</sup>J<sub>P(4),Pt(2)</sub> = 22 Hz, <sup>2</sup>J<sub>P(4),P(4)</sub> = 170 Hz, <sup>3</sup>J<sub>P(4),P(3)</sub> = 10 Hz, <sup>3</sup>J<sub>P(4),P(1)</sub> = 8 Hz, <sup>2</sup>J<sub>P(4),P(1)</sub> = 260 Hz, <sup>3</sup>J<sub>P(4),P(2)</sub> = 35 Hz) ppm.

<sup>195</sup>Pt{<sup>1</sup>H} NMR (CD<sub>2</sub>Cl<sub>2</sub>, 298 K, δ): -5019 (broad, Pt<sup>1</sup>, <sup>1</sup>J<sub>Pt(1),P(4)</sub> = 2434 Hz, <sup>2</sup>J<sub>Pt(1),P(4)</sub> = 2002 Hz), -5630 (broad, Pt<sup>2</sup>, <sup>1</sup>J<sub>Pt(2),P(1)</sub> = 1816 Hz, <sup>1</sup>J<sub>Pt(2),P(2)</sub> = 2828 Hz, <sup>1</sup>J<sub>Pt(2),P(3)</sub> = 3363 Hz) ppm.



## ASSOCIATED CONTENT

**Supporting Information.** <sup>31</sup>P{<sup>1</sup>H} NMR spectra of [2-H<sub>2</sub>O][BF<sub>4</sub>]<sub>2</sub>, [2-CH<sub>3</sub>CN][BF<sub>4</sub>]<sub>2</sub>, [2-PhCN][BF<sub>4</sub>]<sub>2</sub>, [2-PPh<sub>3</sub>][BF<sub>4</sub>]<sub>2</sub>, and [9][BF<sub>4</sub>]<sub>2</sub>; <sup>1</sup>H{<sup>31</sup>P} NMR spectrum of [9][BF<sub>4</sub>]<sub>2</sub>; <sup>1</sup>H-<sup>195</sup>Pt HMQC spectra of [2-H<sub>2</sub>O][BF<sub>4</sub>]<sub>2</sub>, [2-CH<sub>3</sub>CN][BF<sub>4</sub>]<sub>2</sub>, [2-PhCN][BF<sub>4</sub>]<sub>2</sub>, [2-PPh<sub>3</sub>][BF<sub>4</sub>]<sub>2</sub>, and [9][BF<sub>4</sub>]<sub>2</sub>; <sup>1</sup>H EXSY spectrum of [2-H<sub>2</sub>O][BF<sub>4</sub>]<sub>2</sub>; MS data of [2-H<sub>2</sub>O][BF<sub>4</sub>]<sub>2</sub>, [2-CH<sub>3</sub>CN][BF<sub>4</sub>]<sub>2</sub>, [2-PPh<sub>3</sub>][BF<sub>4</sub>]<sub>2</sub>, and **8**; NMR features of [2-BF<sub>3</sub>OH][BF<sub>4</sub>]<sub>2</sub>, [5]<sup>+</sup>, [2-acetone-*d*<sub>6</sub>][BF<sub>4</sub>]<sub>2</sub>, [2-CD<sub>2</sub>Cl<sub>2</sub>][BF<sub>4</sub>]<sub>2</sub>, [3-CH<sub>3</sub>CN][BF<sub>4</sub>]<sub>2</sub>, and [6<sup>+</sup>](Y); crystallographic data in CIF format for the structural analyses of [2-CH<sub>3</sub>CN][BF<sub>4</sub>]<sub>2</sub> and [9][BF<sub>4</sub>]<sub>2</sub> · 2CH<sub>2</sub>Cl<sub>2</sub>. This material is available free of charge via the Internet at <http://pubs.acs.org>.

## AUTHOR INFORMATION

### Corresponding Author

\*E-mail: p.mastrorilli@poliba.it.

## ACKNOWLEDGMENT

Dr. A. Sibouh and Prof. T. Repo (University of Helsinki, FI, HRMS) and Dr. Andrea Raffaelli (CNR ICCOM, UOS of Pisa, IT, MS/MS) are gratefully acknowledged for the mass spectrometry analyses. COST Phosphorus Science Network (PhoSciNet, project CM0802) is gratefully acknowledged for financial support.

## REFERENCES

- Gallo, V.; Latronico, M.; Mastrorilli, P.; Nobile, C. F.; Suranna, G. P.; Ciccarella, G.; Englert, U. *Eur. J. Inorg. Chem.* **2005**, 4607–4616.
- Gallo, V.; Mastrorilli, P.; Polini, F.; Latronico, M.; Re, N.; Englert, U. *Inorg. Chem.* **2008**, *47*, 4785–4795.
- Latronico, M.; Polini, F.; Gallo, V.; Mastrorilli, P.; Calmuschi-Cula, B.; Englert, U.; Re, N.; Repo, T.; Raisanen, M. *Inorg. Chem.* **2008**, *47*, 9779–9796.
- Mastrorilli, P.; Latronico, M.; Gallo, V.; Polini, F.; Re, N.; Marrone, A.; Gobetto, R.; Ellena, S. *J. Am. Chem. Soc.* **2010**, *132*, 4752–4765.
- For P(OH)Cy<sub>2</sub>, see ref 2; for HCl, HBr, HI, PhOH, CF<sub>3</sub>CH<sub>2</sub>OH, and PhSH, see ref 3.
- A similar six-membered platinum cycle was invoked as an intermediate in the H<sub>2</sub> addition to **1**: see ref 4.
- The disappearance of the POH and H<sub>2</sub>O signals upon D<sub>2</sub>O addition is immediate, whereas 2 h are required for complete disappearance of the μ-H signal.
- In fact, the protonation reaction with HCl or HBr is reversible, as **1** is quantitatively reformed by reaction of the protonated species with NaOH.<sup>2</sup> A theoretical treatment of the acidic character of the bridging hydrides can be found in ref 2 and refs therein.
- Wamser, C. A. *J. Am. Chem. Soc.* **1948**, *70*, 1209–1215.
- Main NMR features for [2-B(OH)F<sub>3</sub>][BF<sub>4</sub>] are given as Supporting Information.
- NMR data for [5]<sup>+</sup> are given as Supporting Information.
- An analogous behavior has been reported for the protonation of [(PPh<sub>3</sub>)Pt(μ-C<sub>6</sub>H<sub>4</sub>(PPh<sub>2</sub>)<sub>2</sub>)(μ-PPH<sub>2</sub>)Pt(PPh<sub>3</sub>)] (Pt–Pt): Archambault, C.; Bender, R.; Braunstein, P.; Dusausoy, Y. *Dalton Trans.* **2002**, 4084–4090.

(13) Ara, I.; Chaouche, N.; Forniés, J.; Fortuño, C.; Kribii, A.; Martín, A. *Eur. J. Inorg. Chem.* **2005**, 3894–3901.

(14) Albinati, A.; Bracher, G.; Carmona, D.; Jans, J. H. P.; Klooster, W. T.; Koetzle, T. F.; Macchioni, A.; Ricci, J. S.; Thouvenot, R.; Venanzi, L. M. *Inorg. Chim. Acta* **1997**, *265*, 255–265.

(15) Spek, A. L. *J. Appl. Crystallogr.* **2003**, *36*, 7–13.

(16) NMR data for [3-CH<sub>3</sub>CN]<sup>+</sup> are given as Supporting Information.

(17) Due to the low affinity of F for Pt, only a few fluoro or bifluoro Pt complexes are known: (a) Hintermann, L. H.; Lång, F.; Maire, P.; Togni, A. *Eur. J. Inorg. Chem.* **2006**, 1397–1412. (b) Yahav, A.; Goldberg, I.; Vigalok, A. *Inorg. Chem.* **2005**, *44*, 1547–1553 and refs therein. (c) Yahav, A.; Goldberg, I.; Vigalok, A. *J. Am. Chem. Soc.* **2003**, *125*, 13634–13635. (d) Jasim, N. A.; Perutz, R. N. *J. Am. Chem. Soc.* **2000**, *122*, 8685–8693. (e) Hintermann, S.; Pregosin, P. S.; Rüegger, H.; Clark, H. C. *J. Organomet. Chem.* **1992**, *435*, 225–234.

(18) Only broadening of the <sup>31</sup>P{<sup>1</sup>H} NMR signals was observed, as reported in ref 2.

(19) It is known that fluoride ions exist in solution solvated by hydrogen bond donors: (a) Giguère, P. A. *Chem. Phys. Lett.* **1976**, *41*, 598–600. (b) Giguère, P. A.; Turrell, S. *Can. J. Chem.* **1976**, *54*, 3477–3482. (c) Braddy, R.; McTigue, P. T.; Verity, B. *J. Fluor. Chem.* **1994**, *66*, 63–67. (d) Shenderovich, I. G.; Smirnov, S. N.; Denisov, G. B.; Gindin, V. A.; Golubev, N. S.; Dunger, A.; Reibke, R.; Kirpekar, S.; Malkina, O. L.; Limbach, H.-H. *Ber. Bunsenges. Phys. Chem.* **1998**, *102*, 422–428.

(20) Such a behavior has been already observed passing from [(Cy<sub>2</sub>PH)(Cl)Pt(μ-PCy<sub>2</sub>)(μ-H)Pt(Cy<sub>2</sub>PH){κP-P(OH)Cy<sub>2</sub>}]Cl (Pt–Pt) ([2-Cl]Cl) to [(Cy<sub>2</sub>PH)(Cl)Pt(μ-PCy<sub>2</sub>)(μ-H)Pt(Cy<sub>2</sub>PH){κP-P(OH)Cy<sub>2</sub>}] [BF<sub>4</sub>] (Pt–Pt) ([2-Cl][BF<sub>4</sub>]). See ref 2.

(21) Mastrorilli, P. *Eur. J. Inorg. Chem.* **2008**, 4835–4850 and refs therein.

(22) Leoni, P.; Pasquali, M.; Fortunelli, A.; Germano, G.; Albinati, A. *J. Am. Chem. Soc.* **1998**, *120*, 9564–9573.

(23) The same reactivity was observed reacting **8** with HCl, which led to the soluble species [9]Cl<sub>2</sub>.

(24) The clathrated dichloromethane is held responsible for the signal at δ 5.73 in the <sup>1</sup>H NMR spectrum recorded in dms-*d*<sub>6</sub>.

(25) Dell'Anna, M. M.; Englert, U.; Latronico, M.; Luis, P. L.; Mastrorilli, P.; Giardina Papa, D.; Nobile, C. F.; Peruzzini, M. *Inorg. Chem.* **2006**, *45*, 6892–6900.

(26) Ara, I.; Chaouche, N.; Forniés, J.; Fortuño, C.; Kribii, A.; Tsipis, A. C. *Organometallics* **2006**, *25*, 1084–1091.

(27) (a) Forniés, J.; Fortuño, C.; Navarro, R.; Martínez, F.; Welch, A. J. *J. Organomet. Chem.* **1990**, *394*, 643–658. (b) Forniés, J.; Fortuño, C.; Gil, R.; Martín, A. *Inorg. Chem.* **2005**, *44*, 9534–9541.

(28) (a) Falvello, L.; Forniés, J.; Fortuño, C.; Martín, A.; Martínez-Sariñena, A. P. *Organometallics* **1997**, *16*, 5849–5856. (b) Alonso, E.; Forniés, J.; Fortuño, C.; Martín, A.; Orpen, A. G. *Organometallics* **2000**, *19*, 2690–2697. (c) Alonso, E.; Forniés, J.; Fortuño, C.; Martín, A.; Orpen, A. G. *Organometallics* **2003**, *22*, 2723–2728.

(29) Fărcașiu, D.; Ghenciu, A. *Prog. Nucl. Magn. Reson. Spectrosc.* **1996**, *29*, 129–168.

(30) Cotton, F. A.; Wilkinson, G. *Advanced Inorganic Chemistry*, 5th ed.; Wiley: New York, 1988.

(31) NMR data for [6<sup>+</sup>] are given as Supporting Information.

(32) Carlton, L. *Bruker Report* **2000**, *148*, 28–29.

(33) (a) Amsterdam Density Functional (ADF); SCM, Theoretical Chemistry, Vrije Universiteit, Amsterdam, Netherlands 2004 ([www.scm.com](http://www.scm.com)). (b) Boerrigter, P. M.; te Velde, G.; Baerends, E. *J. Int. Quantum Chem.* **1988**, *33*, 87–113. (c) te Velde, G.; Baerends, E. *J. Chem. Phys.* **1992**, *99*, 84–98.

(34) Vosko, S. H.; Wilk, L.; Nusair, M. *Can. J. Phys.* **1980**, *58*, 1200–1211.

(35) Becke, A. D. *Phys. Rev. A* **1988**, *38*, 3098–3100.

(36) Perdew, J. P. *Phys. Rev. B* **1986**, *33*, 8822–8824.

(37) (a) Lenthe, E. V.; Baerends, E. J.; Snijders, J. G. *J. Chem. Phys.* **1993**, *99*, 4597–4610. (b) Lenthe, E. V.; Baerends, E. J.; Snijders, J. G. *J. Chem. Phys.* **1994**, *101*, 9783–9792.

(38) (a) Minori, A.; Sayaka, M.; Takahito, N.; Kimihiko, H. *Chem. Phys.* **2005**, *311*, 129–137. (b) Xia, F.; Chen, J.; Cao, Z. X. *Chem. Phys. Lett.* **2006**, *418*, 386–391.

(39) Klamt, A.; Schüürmann, G. *J. Chem. Soc., Perkin Trans.* **1993**, *2*, 799–805.

(40) Pye, C. C.; Ziegler, T. *Theor. Chem. Acc.* **1999**, *101*, 396–408.

(41) Crystallographic data (excluding structure factors) for [9][BF<sub>4</sub>]<sub>2</sub>·2CH<sub>2</sub>Cl<sub>2</sub> and [2-CH<sub>3</sub>CN][BF<sub>4</sub>]<sub>2</sub> have been deposited with the Cambridge Crystallographic Data Centre as supplementary publication nos. CCDC 803464 ([9][BF<sub>4</sub>]<sub>2</sub>·2CH<sub>2</sub>Cl<sub>2</sub>) and CCDC 803463 ([2-CH<sub>3</sub>CN][BF<sub>4</sub>]<sub>2</sub>). Copies of the data can be obtained free of charge on application to CCDC, 12 Union Road, Cambridge CB2 1EZ, U.K. [Fax: int. code + 44(1223)336–033; E-mail: deposit@ccdc.cam.ac.uk].

(42) Sheldrick, G. M. *SADABS, Program for Empirical Absorption Correction of Area Detector Data*; University of Göttingen: Göttingen, Germany, 1996.

(43) Sheldrick, G. M. *Acta Crystallogr., Sect. A* **2008**, *64*, 112–122.

(44) The fine structure of this signal was observable in the presence of strong excess HBF<sub>4</sub>, when the exchange rate of the POH was relatively low.